IEEE Access
Multidisciplinary ⋮ Rapid Review ⋮ Open Access Journal

Received August 20, 2020, accepted September 2, 2020, date of publication September 10, 2020,
date of current version September 21, 2020.

Digital Object Identifier 10.1109/ACCESS.2020.3023163

Uplink and Downlink NOMA Transmission Using Full-Duplex UAV

DINH-THUAN DO[1], (Senior Member, IEEE), TU-TRINH THI NGUYEN[2], TU N. NGUYEN[3], (Senior Member, IEEE), XINGWANG LI[4], (Senior Member, IEEE), AND MIROSLAV VOZNAK[5], (Senior Member, IEEE)

[1]Wireless Communications Research Group, Faculty of Electrical & Electronics Engineering, Ton Duc Thang University, Ho Chi Minh City 700000, Vietnam
[2]Faculty of Electronics Technology, Industrial University of Ho Chi Minh City, Ho Chi Minh City 700000, Vietnam
[3]Department of Computer Science, Purdue University Fort Wayne, Fort Wayne, IN 46805, USA
[4]School of Physical and Electronics Engineering, Henan Polytechnic University, Jiaozuo 454000, China
[5]Faculty of Electrical Engineering and Computer Science, Technical University of Ostrava, 70833 Ostrava, Czech Republic

Corresponding author: Dinh-Thuan Do (dodinhthuan@tdtu.edu.vn)

This work was supported by the Czech Ministry of Education, Youth, and Sports, conducted at the VSB–Technical University of Ostrava, under Grant SP2020/65.

ABSTRACT In this article, an unmanned aerial vehicle (UAV)-aided non-orthogonal multiple access (NOMA) network along with uplink (UL) and downlink (DL) transmissions is investigated. A group of sources intend to communicate with a group of destinations over Nakagami-*m* fading channels. Decode-and-Forward (DF) protocol is adopted at the relay (UAV plays the role of relay) while successive interference cancellation (SIC) is required at destinations (receivers) for signal detection, e.g., imperfect SIC (ipSIC) and perfect SIC (pSIC) are studied. The UAV relay benefits from the modes of full-duplex/half-duplex (FD/HD). We then derive analytical expressions of outage probability as main metric. Simulations are conducted to valid the analytical expressions. Moreover, the levels of the effectiveness of the FD mode and pSIC case are demonstrated through analysis and simulation and then compared with those of their counterparts. Numerical results are presented to validate the effectiveness of the proposed UAV-aided NOMA transmission strategies.

INDEX TERMS Full-duplex, non-orthogonal multiple access, unmanned aerial vehicle, outage probability, throughput.

I. INTRODUCTION

In order to accommodate the explosive increase in data traffic of mobile devices, various transmission protocols in wireless networks and mobile networking techniques have been developed. Recently, technical evolution in the scope of massive connections has drawn great attention from the research community and industry. In order to support the tremendous demand for data traffic, a promising multiple access technique, namely non-orthogonal multiple access (NOMA) scheme. Such a technique benefits the mobile networking techniques by enabling massive connections for 5G mobile networks. The NOMA is known as exploiting the power domain into a new dimension to distinguish different users [1] and exhibits increased spectral efficiency over conventional orthogonal multiple access (OMA) scheme, e.g., TDMA/FDMA/CDMA schemes [3]. Unlike the well-known water-filling scheme, the system relying on NOMA allocates more power to users under weaker channel condition and thus maintains user fairness [4]. As a result, the NOMA system achieves larger total throughput and low latency of both uplink and downlink as compared to the OMA scheme [5], [6]. Such features of the NOMA make itself an attractive option for 5G networks and a serious competitor to other well-known schemes such as the orthogonal frequency division multiple access (OFDMA) [8].

Following the principle of the NOMA scheme, a large number of users can simultaneously access the same channel by employing superposition coding at the transmitter and successive interference cancellation (SIC) at the receiver. To exploit the benefit from spatial diversity, cooperative relaying has been explored. In general, relay network where the transmitter and receiver are interconnected by means of relay node has been introduced as an efficient

The associate editor coordinating the review of this manuscript and approving it for publication was Mauro Fadda.

way to extend the coverage and to overcome channel fading and path loss. The relay network can be classified into non-regenerative network and regenerative network. The relay of non-regenerative network operates in non-regenerative mode and the amplify-and-forward (AF) mode belongs to the non-regenerative mode. On the other hand, the relay of regenerative network regenerates the received signal by decoding followed by forwarding. The decode-and-forward (DF) mode is known as a regenerative mode, i.e. firstly decodes received signal and then re-transmits decoded signal to the destination. Lately, various works on the performance of cooperative relay network combined with the NOMA scheme have appeared in the literature [9]–[14]. Spatial multiplexing in cooperative relay network combined with the NOMA is presented in [15] to improve the spectral efficiency. To gain an insight into the successive interference cancellation (SIC), a relay network relying on NOMA has been studied in [16] and the important metrics such as ergodic sum rate with two SIC scenarios has been considered in [16].

A. RELATED WORK

The full-duplex (FD) communication mode in relay networks [17], [18] is important for future wireless networks. By allowing simultaneous transmission and reception on the same frequency channel, the FD communication mode can enhance the spectral efficiency of wireless networks. However, because of self-interference, significant performance degradation can incur and due to imperfect RF chain isolation elimination of the signal leakage becomes challenging. The concept of relay network applied to the NOMA scheme leads to form cooperative NOMA scheme, where the near users that are close to the base station (BS) and thus in better channel conditions are used as relays to help the far users in poor channel conditions. Due to spectral efficiency of the FD communication mode and the flexibility in re-configuring relay networks, the FD communication can be in-cooperated with NOMA [19]. Recently, NOMA has been applied in the air-to-ground (A2G) communication system to improve the system performance [19]. For UAV-assisted mobile communication systems, UAV can serve as an aerial BS to offload part of the traffic from a heavy-crowded multiple access cellular network to improve the quality of service (QoS). Moreover, UAV can act as a flying cellular-connected user equipment (UE) such as cargo delivery applications or even a mobile relay to transfer data between two widely-separated end-points [20]. Regarding to multi-antenna UAV, a general multiple input multiple output (MIMO) NOMA UAV-aided network was proposed in [21]. They derived formula of the sum rate and outage performance of UAV-assisted network. Authors in [22] further considered the physical limitations of the antenna array and introduce the beam scanning to enhance the sum rate performance. In a cellular-connected UAV network, the concurrent uplink is enabled for transmission between the aerial user equipment (AUE) and a terrestrial user equipment (TUE) by implementing NOMA [23]. They considered the rate coverage probability which is known as the probability that the achievable rate of both the AUE and TUE exceeds the expected rates. In [24], NOMA multi-way relaying networks are studied to allow multiple terrestrial users exchange their mutual information via an AF-based UAV relay. The authors derived the analytical expressions for the achievable sum-rate. A model of dual-diversity receivers on UAVs is applied in a NOMA-aided UAV system and bivariate Rician shadowed fading channels are adopted [25]. Regarding promising applications of UAV, a UAV relay is more efficient in an emergency circumstance due to providing backhaul links to perform signals exchange. While a ground relay in a disaster area is likely destroyed in a harsh environment. As an advantage, a UAV relay with its high altitude is free from dangerous situations in the ground. Furthermore, a higher UAV altitude provides a better LoS propagation channel, which makes the AtG link benefit to current cellular systems and enhance the channel performance. Therefore, communication services are still be served in an emergency situation by enabling a UAV serving as an aerial relay. In particular, the authors in [26]- [33] investigated promising applications related NOMA, UAV, vehicle to everything (V2X). For example, [26] studied NOMA-enabled mobile relaying. In their study, to serve as a mobile decode-and-forward (DF) relay, a fixed-wing UAV flies in a circular trajectory to guarantee a reliable link. In [31], the authors considered a full duplex NOMA (FD-NOMA)-based decentralized V2X system model and to meet the requirements of massively connected devices, different quality of services (QoS).

B. MOTIVATION AND OUR CONTRIBUTIONS

In the foregoing scenarios of NOMA scheme, Rayleigh flat fading channel model is typically considered for performance evaluation. In our work, the performance of FD-NOMA scheme over general wireless channels is represented by exploiting Nakagami-m fading. It is pointed out that the Gaussian channel is a special case of the Nakagami channel with the fading parameter $m = 1/2$ and the Rayleigh fading channel is a particular case with the fading parameter $m = 1$. Indeed, very few works studied the performance of FD-NOMA scheme for UAV system over the Nakagami-m fading channel. Although [26], [27] considered uplink downlink NOMA-assisted UAV system, however it is necessary to investigate the fundamental impact of communication channel on the performance of UAV system over Nakagami-m channel. Therefore, this article provides a general framework to design uplink downlink NOMA-assisted UAV in practice. This work also shows the relative performance of the FD-NOMA scheme over the HD-NOMA scheme and a comparison with result reported in [28] is further considered.

The main contributions of this article are as follows

- Different from [23]- [26], this study presents a FD UAV for uplink-downlink (UL-DL) in the scenario of NOMA (termed as FD UL-DL NOMA assisted UAV system), wherein two sources are able to communicate

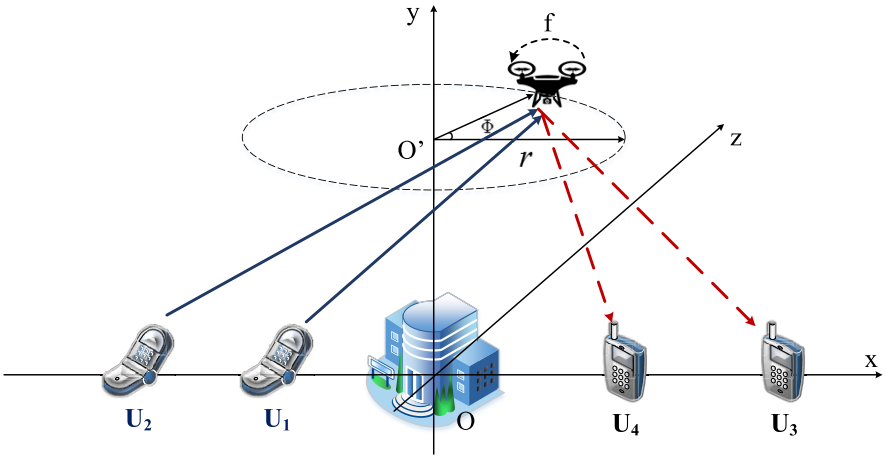

FIGURE 1. System model of UL-DL UAV system relying on NOMA.

simultaneously with their corresponding destinations via an FD-aided UAV over Nakagami-*m* fading channels. Unlike other published work dealing with the FD-NOMA scheme over specific type of communication channel such as the Rayleigh fading channel, our work provides generalized performance evaluation of the FD UL-DL NOMA-assisted UAV system in the presence of Nakagami-*m* channels.

- The closed-form expressions of outage probability for the HD-NOMA and FD-NOMA modes are derived. Since they are formulated in terms of various system parameters, the effect of each system parameter on the outage probability can be numerically evaluated. For instance, the effect of ipSIC on the outage probability can be evaluated to how the system works in practice. It is demonstrated in this work that the outage probability of the system relying on FD-NOMA mode is lower than that of HD-NOMA mode.
- It can be concluded by analysis and simulation that the system relying on FD-NOMA scheme can achieve optimal outage performance with specific power allocation factor, self-interference level, and the transmit SNR at sources. Such optimal outage performance achieved with selected values of system parameters provides the guideline to design UAV system with highly efficient.
- The derivation of asymptotic outage probability also provides an important evaluation to design such UAV system. Compared with OMA-assisted UAV system, the considered system exhibits more benefits and it becomes prominent candidate to implement in practice.
- The comparison between our work with results reported in [28] in terms of outage probabilities provides an important insight on the behavior of these schemes according to specific evaluation criteria. Although a few work studied similar system model with our work, but such comparison is necessary to evaluate benefits of the considered UAV system.

The remainder of this article is structured as follows. In Section II, the system model of the NOMA-assisted UAV system is introduced and UL-DL mechanism between two user pairs is mathematically described. In Section III, the closed-form expressions of outage probability are derived for the UAV system relying on HD-NOMA and FD-NOMA schemes operating over Nakagami-*m* channels. In Section IV, the system model in HD mode and throughput performance in delay limited transmission mode is established. In Section V, we derive the approximated form of outage probability in the considered system. Section VI gives simulation results and corresponding performance analysis, followed by conclusions and future directions in Section VII.

II. SYSTEM MODEL

A. SYSTEM ARCHITECTURE

Consider a scenario where two sources transmit signals to two different destinations via an intermediate UAV relay, which is shown as Fig. 1. In this scenario, the UAV operates as a relay to assist a group of transmitters which are distributed in one place intending to communicate with their corresponding destinations distributed in another place.[1] In this case, poor channel conditions and/or physical obstructions are the main reasons for the lack of direct transmission between sources and destinations. Considering an ideal situation, a perfect Decode and Forward (DF) mode is required to exactly decode the signal at the UAV. Now, the question is: how can a common relay help in multiple access for the UL and DL? To answer this difficult question, the following system and channel models are proposed in this study.

First, a DF scheme and FD mode are jointly deployed at a UAV that performs the role of communication link serving two source-destination pairs, as in Fig. 1. The first

[1] As previous work [26], [27], we limit of our consideration on the two pairs of users. Similar analysis can be achieved for the case of high number of users.

group contains U_1, U_3 while U_2, U_4 belong to the second group; these users employ the NOMA mechanism. It should be noted that U_1, U_2 transmit their signals simultaneously to the distant users, i.e. U_3, U_4, but each dual-hop transmission corresponds to UL (first hop) and DL (second hop).

In this scenario, the signal processing procedure occurs in two hops of the relaying network corresponding the two time slots. To handle uplink transmission for such a NOMA-assisted UAV system, both source nodes U_1, U_2 simultaneously transmit signals x_1, x_2, respectively, in the first hop; this is performed during the considered first time slot. We denote h_1, h_2 as two channels that serve the uplink NOMA. Transmission from the UAV to the destination in the second hop is considered as downlink and these channels are denoted by g_1, g_2. It is assumed these channel follow the general Nakagami-m distribution [24]. In the FD scenario, to represent residual self-interference, we denote f as a self-interference channel among transmit/receive antenna pairs equipped at the UAV. Regarding the ipSIC, interference channels are denoted as k_r, k_2. In the first phase, the allocated power factors are $\upsilon_1 P$, $\upsilon_2 P$ so as to distinguish power levels for the two symbols, i.e. x_1, x_2, corresponding to separated services for the first phase; $\upsilon_3 P_R$, $\upsilon_4 P_R$ are re-assigned as allocated power for the two symbols in the second transmission phase, where $\upsilon_1, \upsilon_2, \upsilon_3, \upsilon_4$ are the power allocation coefficients (PACs); finally, P, P_R in this consideration are the total transmit power at the transmitters and the relay, respectively. Concurrently, the superimposed signal $\sqrt{P_R \upsilon_3} x_1 + \sqrt{P_R \upsilon_4} x_2$ is re-transmitted by the relay to U_3, U_4. It is worth noting that such a UAV can operate in FD mode which leads to processing delay with small time epoch. The constraint of power allocation fractions in NOMA are $\upsilon_1 + \upsilon_2 = 1$, $\upsilon_3 + \upsilon_4 = 1$ and their assignments have significant impacts on system performance [27]. Relying on NOMA, SIC is required at both UAV and destination to detect remaining signals; the two cases need to be considered carefully, i.e. ipSIC and pSIC. For positioning of UAV and NOMA users, we consider three dimensional Cartesian coordinates (x, y, z). First, we present the location of the sources U_1, U_2 at $U_1\left(-x_{U_1}, 0, 0\right)$, $U_2\left(-x_{U_2}, 0, 0\right)$ with respect to the origin. The locations of destinations U_3, U_4 are $U_3\left(x_{U_3}, 0, 0\right), U_4\left(x_{U_4}, 0, 0\right)$, respectively. The central location of the circular trajectory of UAV (R) with radius r and altitude h is at coordinates $O'(0, h, 0)$. Considering Φ as the angle of the circle of UAV location with respect to the x-axis, we can readily represent the location of R at $R\left(r\sin\left(\frac{\pi}{2}-\Phi\right), h, \cos\left(\frac{\pi}{2}-\Phi\right)\right)$.

Based on the analysis, we can achieve the Euclidean distances from U_1, U_2 to R and from R to U_3, U_4, are given respectively as $d_{U_1R} = \sqrt{r^2 + h^2 + x_{U_1}^2 + 2rx_{U_1}\sin\left(\frac{\pi}{2}-\Phi\right)}$, $d_{U_2R} = \sqrt{r^2 + h^2 + x_{U_2}^2 + 2rx_{U_2}\sin\left(\frac{\pi}{2}-\Phi\right)}$, $d_{RU_3} = \sqrt{r^2 + h^2 + x_{U_3}^2 - 2rx_{U_3}\sin\left(\frac{\pi}{2}-\Phi\right)}$, and $d_{RU_4} = \sqrt{r^2 + h^2 + x_{U_4}^2 - 2rx_{U_4}\sin\left(\frac{\pi}{2}-\Phi\right)}$.

B. SIGNAL-TO-NOISE RATIO (SNR) CALCULATION

We first consider FD mode for UL NOMA, x_1 is first decoded at the UAV relay to obtain a better channel condition. Then, x_1 is considered to be noise, and indicates poor channel condition..[2] The received signal at UAV relay can be given as

$$y_R = \upsilon_1\sqrt{P_S}h_1x_1 + \upsilon_2\sqrt{P_S}h_2x_2 + \eta_R, \tag{1}$$

where η_R is AWGN noise term, σ_0^2 is assumed to be noise variance for all noise terms.

Therefore, the signal to interference plus noise ratio (SINR) to detect x_1 at relay can be formulated similar to [25] and it is given as

$$\gamma_{R\leftarrow 1} = \frac{\upsilon_1\rho_S|h_1|^2}{\upsilon_2\rho_S|h_2|^2 + \rho_R|f|^2 + 1}, \tag{2}$$

where $\rho_S \triangleq P/\sigma_0^2$ is the transmit signal to noise ratio (SNR) of source. Similarly, in HD mode, the SINR is rewritten as

$$\gamma_{R\leftarrow 1}^{HD} = \frac{\upsilon_1\rho_S|h_1|^2}{\upsilon_2\rho_S|h_2|^2 + 1}, \tag{3}$$

At the UAV, to detect signal x_2, the operation of SIC is required; it is then carried out at the UAV to help in detection. In a pSIC situation, the SNR at the relay node to decode x_2 is determined in FD mode by

$$\gamma_{R\leftarrow 2}^{pSIC} = \frac{\upsilon_2\rho_S|h_2|^2}{\rho_R|f|^2 + 1}. \tag{4}$$

In HD mode, the SNR is expressed by

$$\gamma_{R\leftarrow 2}^{pSIC,HD} = \upsilon_2\rho_S|h_2|^2. \tag{5}$$

When ipSIC occurs at the considered UAV system, these expressions can be recomputed respectively as

$$\gamma_{R\leftarrow 2}^{ipSIC} = \frac{\upsilon_2\rho_S|h_2|^2}{\upsilon_1\rho_S|k_r|^2 + \rho_R|f|^2 + 1}, \tag{6}$$

and

$$\gamma_{R\leftarrow 2}^{ipSIC,HD} = \frac{\upsilon_2\rho_S|h_2|^2}{\upsilon_1\rho_S|k_r|^2 + 1}, \tag{7}$$

where $k_r \sim \Gamma\left(m_{k_r}, \beta_{k_r}\right)$ is an interference term related to ipSIC; $\rho_R \triangleq P_R/\sigma_0^2$ is the transmit SNR at the UAV.
The received signal at destinations U_3 and U_4 can be expressed as follow

$$y_{U_n} = \upsilon_3\sqrt{P_R}g_1x_1 + \upsilon_4\sqrt{P_R}g_2x_2 + \eta_{U_n}. \tag{8}$$

Regarding the second hop transmission, the destination intends to decode its own data and hence the SINR can be achieved at destination U_3 by

$$\gamma_{U_3} = \frac{\upsilon_3\rho_R|g_1|^2}{\upsilon_4\rho_R|g_1|^2 + 1}. \tag{9}$$

[2]Similar as recent work, the synchronization technique to transmit x_1, x_2 from two sources is beyond the scope of our paper [27].

However, signal of destination U_3 is considered as noise at destination U_4 which intends to eliminate noise before detecting its own signal; hence, SINR can be achieved at destination U_4 as

$$\gamma_{U_4 \leftarrow 1} = \frac{\upsilon_3 \rho_R |g_2|^2}{\upsilon_4 \rho_R |g_2|^2 + 1}. \tag{10}$$

Additionally, destination U_4 can decode its information after successful extraction of signal at U_3 data and application of SIC. Then, SNR and SINR at the second destination in the two cases including pSIC and impSIC, are given respectively as

$$\gamma_{U_4}^{pSIC} = \upsilon_4 \rho_R |g_2|^2, \tag{11}$$

and

$$\gamma_{U_4}^{ipSIC} = \frac{\upsilon_4 \rho_R |g_2|^2}{\upsilon_3 \rho_R |k_2|^2 + 1}. \tag{12}$$

III. OUTAGE PERFORMANCE IN FULL-DUPLEX MODE

As an important metric, this section presents outage probability in a system containing links over an independent Nakagami-m fading channel. To evaluate system performance, our goal is to present outage behavior and main results in terms of analytical derivations. It should be mentioned that the outage probability of an ipSIC is the worst case that can be provided. In other words, the different scenarios in such NOMA including HD, FD, pSIC and ipSIC are determined carefully.

A. OUTAGE PROBABILITY OF THE FIRST USER PAIR

The considered system is one that classifies different users with corresponding required quality of service (QoS). In this case, γ_0^1 is assumed to be the predefined SINR thresholds of destination U_3.

Recalling that channel is denoted by $|z|^2$. Since this channel follows a Gamma distribution, we present the probability density function (PDF) and the CDF of $|z|^2$ respectively as

$$f_{|z|^2}(x) = \frac{x^{m_z - 1}}{\Gamma(m_z)\, \beta_z^{m_z}} \exp\left(-\frac{x}{\beta_z}\right), \tag{13}$$

and

$$\begin{aligned} F_{|z|^2}(x) &= 1 - \frac{1}{\Gamma(m_z)} \Gamma\left(m_z, \frac{x}{\beta_z}\right) \\ &= 1 - \exp\left(-\frac{x}{\beta_z}\right) \sum_{n=0}^{m_z - 1} \frac{x^n}{n! \beta_z^n}, \end{aligned} \tag{14}$$

where $f_Z(.)$ and $F_Z(.)$ represent the probability distribution function (PDF) and the cumulative distribution function of random variables (RVs), Z, respectively. The variable β_z is defined as $\beta_z \triangleq \lambda_z / m_z$ with λ_z and m_z representing the mean and integer fading factor. The symbol $\Gamma(.)$ stands for the gamma function.

The first user pair is evaluated according to the outage probability. In this type of NOMA-assisted UAV system, an outage event for the first user pair is explained as: *i) relay cannot decode x_1 correctly; ii) information x_1 cannot be detected by U_3*. In particular, be denoting $\gamma_0^1 = 2^{R_1} - 1$ is required SINR threshold along with target rate R_1, the exact outage probability of the first user pair is given by

$$\begin{aligned} OP_1^{FD} &= \Pr\left(\gamma_{R \leftarrow 1} < \gamma_0^1 \cup \gamma_{U_3} < \gamma_0^1\right) \\ &= 1 - \Pr\left(\gamma_{R \leftarrow 1} \geq \gamma_0^1, \gamma_{U_3} \geq \gamma_0^1\right) \\ &= 1 - \Pr\left(|h_1|^2 \geq \frac{\gamma_0^1}{\upsilon_1 \rho_S}\left(\upsilon_2 \rho_S |h_2|^2 + \rho_R |f|^2 + 1\right)\right) \\ &\quad \times \Pr\left(|g_1|^2 \geq \frac{\gamma_0^1}{\left(\upsilon_3 - \upsilon_4 \gamma_0^1\right) \rho_R}\right), \end{aligned} \tag{15}$$

where $\Pr(.)$ is the outage probability function.

We first introduce a proposition to calculate the outage performance as follow

Proposition 1: The closed-form expression of first user pair in terms of outage probability can be given by

$$\begin{aligned} OP_1^{FD} &= 1 - \Pr\left(|h_1|^2 \geq \frac{\gamma_0^1}{\upsilon_1 \rho_S}\left(\upsilon_2 \rho_S |h_2|^2 + \rho_R |f|^2 + 1\right)\right) \\ &\quad \times \left(1 - F_{|g_1|^2}\left(\frac{\gamma_0^1}{\left(\upsilon_3 - \upsilon_4 \gamma_0^1\right) \rho_R}\right)\right) \\ &= 1 - \exp\left(-\frac{\gamma_0^1}{\upsilon_1 \rho_S \beta_{h_1}}\right) \\ &\quad \times \sum_{n=0}^{m_{h_1} - 1} \sum_{n_1=0}^{n} \sum_{n_2=0}^{n_1} \binom{n}{n_1} \binom{n_1}{n_2} \frac{1}{n! \beta_{h_1}^n} \\ &\quad \times \left(\frac{\gamma_0^1}{\upsilon_1 \rho_S}\right)^n (\rho_R)^{n_2} (\upsilon_2 \rho_S)^{n_1 - n_2} \\ &\quad \times \frac{1}{\Gamma\left(m_f\right) \beta_f^{m_f}} \frac{1}{\Gamma\left(m_{h_2}\right) \beta_{h_2}^{m_{h_2}}} \\ &\quad \times \left(\frac{\gamma_0^1 \rho_R}{\upsilon_1 \rho_S \beta_{h_1}} + \frac{1}{\beta_f}\right)^{-(n_2 + m_f)} \Gamma\left(n_2 + m_f\right) \\ &\quad \times \left(\frac{\gamma_0^1 \upsilon_2}{\upsilon_1 \beta_{h_1}} + \frac{1}{\beta_{h_2}}\right)^{-n_1 + n_2 - m_{h_2}} \\ &\quad \times \Gamma\left(n_1 - n_2 + m_{h_2}\right) \\ &\quad \times \exp\left(-\frac{\gamma_0^1}{\left(\upsilon_3 - \upsilon_4 \gamma_0^1\right) \rho_R \beta_{g_1}}\right) \\ &\quad \times \sum_{n_3=0}^{m_{g_1} - 1} \frac{\left(\gamma_0^1\right)^{n_3}}{n_3! \beta_{g_1}^{n_3} \left(\upsilon_3 - \upsilon_4 \gamma_0^1\right)^{n_3} \rho_R^{n_3}}. \end{aligned} \tag{16}$$

Proof: See Appendix A.

B. OUTAGE PROBABILITY OF THE SECOND USER PAIR WITH ipSIC

In this case, γ_0^2 is assumed to be the predefined SINR thresholds of destination U_4. In a similar way, the second user pair

exhibits outage behavior, as follow

$$OP_2^{ipSIC,FD} = \Pr\left(\begin{matrix}\gamma_{R\leftarrow 1} < \gamma_0^1 \cup \gamma_{R\leftarrow 2}^{ipSIC} < \gamma_0^2 \\ \cup \gamma_{U_4\leftarrow 1} < \gamma_0^1 \cup \gamma_{U_4}^{ipSIC} < \gamma_0^2\end{matrix}\right) = 1 - \underbrace{\Pr\left(\gamma_{R\leftarrow 1} \geq \gamma_0^1, \gamma_{R\leftarrow 2}^{ipSIC} \geq \gamma_0^2\right)}_{\Psi_1} \times \underbrace{\Pr\left(\gamma_{U_4\leftarrow 1} \geq \gamma_0^1, \gamma_{U_4}^{ipSIC} \geq \gamma_0^2\right)}_{\Psi_2}, \quad (17)$$

where $\gamma_0^2 = 2^{R_2} - 1$.

Proposition 2: The closed-form expression of the second user pair in term of outage probability can be computed by

$$OP_2^{ipSIC,FD} = 1 - \Psi_1 \times \Psi_2, \quad (18)$$

in which Ψ_1, Ψ_2 are calculated as shown at the bottom of the page, in (19) and (20) respectively.

Proof: See Appendix B.

C. OUTAGE PROBABILITY OF THE SECOND USER PAIR IN pSIC CASE

In this section, we consider a NOMA-assisted UAV network under the existence of pSIC. In principle, SIC or multilevel decoding can be carried out at the receiver side to extract superimposed messages transmitted from source nodes. In this situation, SIC can be carried out for the same user pair in both the uplink and downlink, and thus the total system capacity can be maximized. Therefore, to ensure optimal communications, it is reasonable to consider the best-case scenario of SIC, in which the residual interference is extremely small.

In such a case, the expressions of outage probability at the second user pair can be rewritten as

$$OP_2^{pSIC,FD} = \Pr\left(\begin{matrix}\gamma_{R\leftarrow 1} < \gamma_0^1 \cup \gamma_{R\leftarrow 2}^{pSIC} < \gamma_0^2 \\ \cup \gamma_{U_4\leftarrow 1} < \gamma_0^1 \cup \gamma_{U_4}^{pSIC} < \gamma_0^2\end{matrix}\right) = 1 - \underbrace{\Pr\left(\gamma_{R\leftarrow 1} \geq \gamma_0^1, \gamma_{R\leftarrow 2}^{pSIC} \geq \gamma_0^2\right)}_{\Psi_3} \times \underbrace{\Pr\left(\gamma_{U_4\leftarrow 1} \geq \gamma_0^1, \gamma_{U_4}^{pSIC} \geq \gamma_0^2\right)}_{\Psi_4}. \quad (21)$$

Next, we provide an extra proposition as below

Proposition 3: Regarding the outage probability, the expression of the second user pair in the pSIC case can be expressed in closed-form by

$$OP_2^{pSIC,FD} = 1 - \Psi_3 \times \Psi_4, \quad (22)$$

$$\begin{aligned}\Psi_1 = {} & \exp\left(-\frac{\gamma_0^1}{\upsilon_1\rho_S\beta_{h_1}}\right)\sum_{n=0}^{m_{h_1}-1}\sum_{n_1=0}^{n}\sum_{n_2=0}^{n_1}\binom{n}{n_1}\binom{n_1}{n_2}\frac{1}{n!\beta_{h_1}^n}\left(\frac{\gamma_0^1}{\upsilon_1\rho_S}\right)^n \\ & \times \exp\left(-\frac{\upsilon_2\gamma_0^1\gamma_0^2}{\upsilon_1\upsilon_2\rho_S\beta_{h_1}} - \frac{\gamma_0^2}{\upsilon_2\rho_S\beta_{h_2}} - \frac{\gamma_0^1}{\upsilon_1\rho_s\beta_{h_1}}\right)\rho_R{}^{n_2}(\upsilon_2\rho_S)^{n_1-n_2} \\ & \times \frac{1}{\Gamma\left(m_{h_2}\right)\beta_{h_2}^{m_{h_2}}}\left(\frac{\gamma_0^1\upsilon_2}{\upsilon_1\beta_{h_1}} + \frac{1}{\beta_{h_2}}\right)^{-n_1+n_2-m_{h_2}}\left(n_1 - n_2 + m_{h_2} - 1\right)! \\ & \times \sum_{n_3=0}^{n_1-n_2+m_{h_2}-1}\sum_{n_4=0}^{n_3}\binom{n_3}{n_4}\binom{n_4}{n_5}\frac{1}{n_3!}\left(\frac{\upsilon_2\gamma_0^1\gamma_0^2}{\upsilon_1\upsilon_2\rho_S\beta_{h_1}} + \frac{\gamma_0^2}{\upsilon_2\rho_S\beta_{h_2}}\right)^{n_3} \\ & \times \Gamma\left(n_2 + n_4 - n_5 + m_f\right)\Gamma\left(n_5 + m_{k_r}\right)\rho_R{}^{n_4-n_5}\upsilon_1{}^{n_5}\rho_S{}^{n_5} \\ & \times \frac{1}{\Gamma\left(m_f\right)\beta_f^{m_f}}\left(\frac{\gamma_0^1\rho_R}{\upsilon_1\rho_S\beta_{h_1}} + \left(\frac{\gamma_0^1\upsilon_2}{\upsilon_1\beta_{h_1}} + \frac{1}{\beta_{h_2}}\right)\frac{\gamma_0^2\rho_R}{\upsilon_2\rho_S} + \frac{1}{\beta_f}\right)^{-(n_2+n_4-n_5+m_f)} \\ & \times \frac{1}{\Gamma\left(m_{k_r}\right)\beta_{k_r}^{m_{k_r}}}\left(\left(\frac{\gamma_0^1\upsilon_2}{\upsilon_1\beta_{h_1}} + \frac{1}{\beta_{h_2}}\right)\frac{\gamma_0^2\upsilon_1}{\upsilon_2} + \frac{1}{\beta_{k_r}}\right)^{-(n_5+m_{k_r})}, \end{aligned} \quad (19)$$

$$\begin{aligned}\Psi_2 = {} & \exp\left(-\frac{\gamma_0^2}{\upsilon_4\rho_R\beta_{g_2}}\right)\sum_{n_6=0}^{m_{g_2}-1}\sum_{n_7=0}^{n_6}\binom{n_6}{n_7}\frac{1}{n_6!\beta_{g_2}^{n_6}}\left(\frac{\gamma_0^2}{\upsilon_4\rho_R}\right)^{n_6}\upsilon_3^{n_7}\rho_R^{n_7} \\ & \times \frac{1}{\Gamma\left(m_{k_2}\right)\beta_{k_2}^{m_{k_2}}}\left(\frac{\gamma_0^2\upsilon_3}{\upsilon_4\beta_{g_2}} + \frac{1}{\beta_{k_2}}\right)^{-(n_7+m_{k_2})}\Gamma\left(n_7 + m_{k_2}, \frac{\gamma_0^2\upsilon_3\vartheta_2}{\upsilon_4\beta_{g_2}} + \frac{\vartheta_2}{\beta_{k_2}}\right) \\ & + \frac{1}{\Gamma\left(m_{g_2}\right)}\Gamma\left(m_{g_2}, \frac{\gamma_0^1}{\left(\upsilon_3 - \gamma_0^1\upsilon_4\right)\rho_R\beta_{g_2}}\right) \times \left(1 - \frac{1}{\Gamma\left(m_{k_2}\right)}\Gamma\left(m_{k_2}, \frac{\vartheta_2}{\beta_{k_2}}\right)\right) \end{aligned} \quad (20)$$

in which,

$$\begin{aligned}\Psi_3 = {} & e^{-\frac{\gamma_0^1}{\upsilon_1\rho_S\beta_{h_1}}-\left(\frac{\gamma_0^1\upsilon_2}{\upsilon_1\beta_{h_1}}+\frac{1}{\beta_{h_2}}\right)\frac{\gamma_0^2}{\upsilon_2\rho_S}} \\ & \times \sum_{n=0}^{m_{h_1}-1}\sum_{n_1=0}^{n}\sum_{n_2=0}^{n_1}\binom{n}{n_1}\binom{n_1}{n_2}\frac{1}{n!\beta_{h_1}^n}\left(\frac{\gamma_0^1}{\upsilon_1\rho_S}\right)^n \\ & \times \rho_R^{n_2}(\upsilon_2\rho_S)^{n_1-n_2}\left(n_1-n_2+m_{h_2}-1\right) \\ & \times \frac{1}{\Gamma\left(m_{h_2}\right)\beta_{h_2}^{m_{h_2}}}\left(\frac{\gamma_0^1\upsilon_2}{\upsilon_1\beta_{h_1}}+\frac{1}{\beta_{h_2}}\right)^{-n_1+n_2-m_{h_2}} \\ & \times \sum_{n_3=0}^{n_1-n_2+m_{h_2}-1}\sum_{n_4=0}^{n_3}\binom{n_3}{n_4}\frac{1}{n_3!} \\ & \times \left(\left(\frac{\gamma_0^1\upsilon_2}{\upsilon_1\beta_{h_1}}+\frac{1}{\beta_{h_2}}\right)\frac{\gamma_0^2}{\upsilon_2\rho_S}\right)^{n_3} \\ & \times \frac{\rho_R^{n_4}}{\Gamma\left(m_f\right)\beta_f^{m_f}}\Gamma\left(n_2+n_4+m_f\right) \\ & \times \left(\frac{\gamma_0^1\rho_R}{\upsilon_1\rho_s\beta_{h_1}}+\frac{\gamma_0^1\gamma_0^2\rho_r}{\upsilon_1\rho_s}+\frac{\gamma_0^2\rho_R}{\beta_{h_2}\upsilon_2\rho_S}+\frac{1}{\beta_f}\right)^{-n_2-n_4-m_f}\end{aligned} \tag{23}$$

and

$$\Psi_4 = \frac{1}{\Gamma\left(m_{g_2}\right)}\Gamma\left(m_{g_2},\frac{1}{\beta_{g_2}}\max\left(\frac{\gamma_0^1}{\left(\upsilon_3-\gamma_0^1\upsilon_4\right)\rho_R},\frac{\gamma_0^2}{\upsilon_4\rho_R}\right)\right) \tag{24}$$

Proof: See Appendix C.

IV. OUTAGE PERFORMANCE IN HALF-DUPLEX MODE AND THROUGHPUT CONSIDERATION

In this section, to enable comparison to the counterpart, HD mode is deployed in our proposed system. Without self-interference due to parallel operation of the dual-antenna at the relay, receivers are required to have lighter signal processing, and hence performance of HD mode still needs to be considered in terms of outage probability. Considering further metrics, throughput performance can be evaluated in two modes, i.e. FD and HD.

A. OUTAGE PERFORMANCE IN HALF-DUPLEX MODE

In this scenario, to examine the first main metric, we consider the outage probability. In particular, outage performance of the first user pair is expressed in HD mode by

$$\begin{aligned}OP_1^{HD} &= \Pr\left(\gamma_{R\leftarrow1}^{HD} < \gamma_{0,HD}^1 \cup \gamma_{U_3} < \gamma_{0,HD}^1\right) \\ &= 1-\Pr\left(\gamma_{R\leftarrow1}^{HD} \geq \gamma_{0,HD}^1, \gamma_{U_3} \geq \gamma_{0,HD}^1\right) \\ &= 1-\Pr\left(\frac{\upsilon_1\rho_S|h_1|^2}{\upsilon_2\rho_S|h_2|^2+1} \geq \gamma_{0,HD}^1\right) \\ &\quad \times \Pr\left(\frac{\upsilon_3\rho_r|g_1|^2}{\upsilon_4\rho_R|g_1|^2+1} \geq \gamma_{0,HD}^1\right),\end{aligned} \tag{25}$$

where $\gamma_{0,HD}^1 = 2^{2R_1}-1$.

After several manipulations, the following proposition can be introduced.

Proposition 4: In HD mode, the outage probability for the first user pair can be formulated in closed-form as

$$\begin{aligned}OP_1^{HD} = {} & 1-e^{-\frac{\gamma_{0,HD}^1}{\upsilon_1\rho_S\beta_{h_1}}-\frac{\gamma_{0,HD}^1}{\left(\upsilon_3-\upsilon_4\gamma_{0,HD}^1\right)\rho_R\beta_{g_1}}} \\ & \times \sum_{n=0}^{m_{h_1}-1}\sum_{n_1=0}^{n}\binom{n}{n_1}\frac{1}{n!}\left(\frac{\gamma_{0,HD}^1}{\upsilon_1\rho_S\beta_{h_1}}\right)^n \\ & \times \upsilon_2^{n_1}\rho_S^{n_1}\Gamma\left(n_1+m_{h_2}\right) \\ & \times \frac{1}{\Gamma\left(m_{h_2}\right)\beta_{h_2}^{m_{h_2}}}\left(\frac{\gamma_{0,HD}^1\upsilon_2}{\upsilon_1\beta_{h_1}}+\frac{1}{\beta_{h_2}}\right)^{-n_1-m_{h_2}} \\ & \times \sum_{n_2=0}^{m_{g_1}-1}\frac{1}{n_2!}\left(\frac{\gamma_{0,HD}^1}{\left(\upsilon_3-\upsilon_4\gamma_{0,HD}^1\right)\beta_{g_1}\rho_R}\right)^{n_2}.\end{aligned} \tag{26}$$

Proof: See Appendix D.

In case of ipSIC, outage probability can be expressed for the second user pair as

$$\begin{aligned}OP_2^{ipSIC,HD} &= \Pr\left(\begin{matrix}\gamma_{R\leftarrow1}^{HD} < \gamma_{0,HD}^1 \cup \gamma_{R\leftarrow2}^{ipSIC,HD} < \gamma_{0,HD}^2 \\ \cup\gamma_{U_4\leftarrow1} < \gamma_{0,HD}^1 \cup \gamma_{U_4}^{ipSIC} < \gamma_{0,HD}^2\end{matrix}\right) \\ &= 1-\underbrace{\Pr\left(\gamma_{R\leftarrow1}^{HD} \geq \gamma_{0,HD}^1, \gamma_{R\leftarrow2}^{ipSIC,HD} \geq \gamma_{0,HD}^2\right)}_{\Psi_5} \\ &\quad \times \underbrace{\Pr\left(\gamma_{U_4\leftarrow1} \geq \gamma_{0,HD}^1, \gamma_{U_4}^{ipSIC} \geq \gamma_{0,HD}^2\right)}_{\Psi_6},\end{aligned} \tag{27}$$

where $\gamma_{0,HD}^2 = 2^{2R_2}-1$.

Therefore, the outage calculation motivates us to introduce the following proposition.

Proposition 5: In terms of the ipSIC case in HD mode, the outage probability for the second user pair can be exactly computed as

$$OP_2^{ipSIC,HD} = 1-\Psi_5\times\Psi_6, \tag{28}$$

in which,

$$\begin{aligned}\Psi_5 = {} & e^{-\frac{\gamma_{0,HD}^1}{\upsilon_1\rho_S\beta_{h_1}}-\frac{\vartheta_1\gamma_{0,HD}^2}{\upsilon_2\rho_S}} \\ & \times \sum_{n=0}^{m_{h_1}-1}\sum_{n_1=0}^{n}\binom{n}{n_1}\frac{\upsilon_2^{n_1}}{n!\rho_S^{n-n_1}}\left(\frac{\gamma_{0,HD}^1}{\upsilon_1\beta_{h_1}}\right)^n \\ & \times \frac{\Gamma\left(\tau_2\right)\vartheta_1{}^{-\tau_2}}{\Gamma\left(m_{h_2}\right)\beta_{h_2}^{m_{h_2}}}\sum_{n_2=0}^{\tau_2-1}\sum_{n_3=0}^{n_2}\binom{n_2}{n_3}\frac{1}{n_2!} \\ & \times \left(\frac{\vartheta_1\gamma_{0,HD}^2}{\upsilon_2\rho_S}\right)^{n_2}\upsilon_1^{n_3}\rho_S^{n_3}\Gamma\left(n_3+m_{k_r}\right) \\ & \times \frac{1}{\Gamma\left(m_{k_r}\right)\beta_{k_r}^{m_{k_r}}}\left(\frac{\upsilon_1\vartheta_1\gamma_{0,HD}^2}{\upsilon_2}+\frac{1}{\beta_{k_r}}\right)^{-n_3-m_{k_r}}\end{aligned} \tag{29}$$

and

$$\Psi_6 = e^{-\frac{\gamma_{0,HD}^2}{\upsilon_4\rho_R\beta_{g_2}}}\sum_{n_6=0}^{m_{g_2}-1}\sum_{n_7=0}^{n_6}\binom{n_6}{n_7}\frac{1}{n_6!\beta_{g_2}^{n_6}} \times \upsilon_3^{n_7}\rho_R^{n_7}\left(\frac{\gamma_{0,HD}^2}{\upsilon_4\rho_R}\right)^{n_6} \times \frac{1}{\Gamma\left(m_{k_2}\right)\beta_{k_2}^{m_{k_2}}}\left(\frac{\gamma_{0,HD}^2\upsilon_3}{\upsilon_4\beta_{g_2}}+\frac{1}{\beta_{k_2}}\right)^{-n_7-m_{k_2}} \times \Gamma\left(n_7+m_{k_2},\left(\frac{\gamma_{0,HD}^2\upsilon_3}{\upsilon_4\beta_{g_2}}+\frac{1}{\beta_{k_2}}\right)\vartheta_2\right) + \frac{1}{\Gamma\left(m_{g_2}\right)}\Gamma\left(m_{g_2},\frac{\gamma_{0,HD}^1}{\left(\upsilon_3-\gamma_{0,HD}^1\upsilon_4\right)\rho_R\beta_{g_2}}\right) \times\left(1-\frac{1}{\Gamma\left(m_{k_2}\right)}\Gamma\left(m_{k_2},\frac{\vartheta_2}{\beta_{k_2}}\right)\right) \tag{30}$$

Proof: See Appendix E.

In a similar way, the outage probability for the second user pair under the ipSIC case can be obtained as follow.

Proposition 6: In HD mode and ipSIC case, the second user pair can be computed in term of outage behavior exactly as

$$OP_2^{pSIC,HD} = \Pr\left(\begin{matrix}\gamma_{R\leftarrow1}^{HD} < \gamma_{0,HD}^1 \cup \gamma_{R\leftarrow2}^{pSIC,HD} < \gamma_{0,HD}^2 \\ \cup\gamma_{U_4\leftarrow1} < \gamma_{0,HD}^1 \cup \gamma_{U_4}^{pSIC} < \gamma_{0,HD}^2\end{matrix}\right) = 1 - \underbrace{\Pr\left(\gamma_{R\leftarrow1}^{HD} \geq \gamma_{0,HD}^1, \gamma_{R\leftarrow2}^{pSIC,HD} \geq \gamma_{0,HD}^2\right)}_{\Psi_7} \times \underbrace{\Pr\left(\gamma_{U_4\leftarrow1} \geq \gamma_{0,HD}^1, \gamma_{U_4}^{pSIC} \geq \gamma_{0,HD}^2\right)}_{\Psi_8}, \tag{31}$$

where

$$\Psi_7 = e^{-\frac{\gamma_{0,HD}^1}{\upsilon_1\rho_S\beta_{h_1}}}\sum_{n=0}^{m_{h_1}-1}\sum_{n_1=0}^{n}\binom{n}{n_1}\frac{\upsilon_2^{n_1}\rho_S^{n_1}}{n!\beta_{h_1}^n}\left(\frac{\gamma_{0,HD}^1}{\upsilon_1\rho_S}\right)^n \times \frac{1}{\Gamma\left(m_{h_2}\right)\beta_{h_2}^{m_{h_2}}}\left(\frac{\gamma_{0,HD}^1\upsilon_2}{\upsilon_1\beta_{h_1}}+\frac{1}{\beta_{h_2}}\right)^{-n_1-m_{h_2}} \times \Gamma\left(n_1+m_{h_2},\left(\frac{\gamma_{0,HD}^1\upsilon_2}{\upsilon_1\beta_{h_1}}+\frac{1}{\beta_{h_2}}\right)\frac{\gamma_{0,HD}^2}{\upsilon_2\rho_S}\right), \tag{32}$$

and

$$\Psi_8 = \frac{1}{\Gamma\left(m_{g_2}\right)}\Gamma\left(\begin{matrix}m_{g_2},\frac{1}{\beta_{g_2}} \\ \times\max\left(\frac{\gamma_{0,HD}^1}{\left(\upsilon_3-\gamma_{0,HD}^1\upsilon_4\right)\rho_R},\frac{\gamma_{0,HD}^2}{\upsilon_4\rho_R}\right)\end{matrix}\right). \tag{33}$$

Similarly, the implicit outage derivation in this proposition can be obtained as for the previously computed position. Due to the simplicity of the analysis, we do not present it here.

B. THROUGHPUT PERFORMANCE IN IN DELAY-LIMITED TRANSMISSION

In this scenario, we consider the throughput in delay-limited transmission for FD and HD NOMA, respectively. In the first scenario related to FD, the throughput of the first user pair corresponding the fixed bit rate R_1 can be computed by

$$A_1^{FD} = \left(1 - OP_1^{FD}\right) \times R_1. \tag{34}$$

Similarly, the throughput of the second user pair corresponding to fixed bit rate R_2 in case of ipSIC will become

$$A_2^{ipSIC,FD} = \left(1 - OP_2^{ipSIC,FD}\right) \times R_2. \tag{35}$$

The sum of the throughput of the system in the case of ipSIC can be computed by

$$A_{sum}^{ipSIC,FD} = \left(1 - OP_1^{FD}\right) \times R_1 + \left(1 - OP_2^{ipSIC,FD}\right) \times R_2. \tag{36}$$

In addition, the throughput of the second user pair corresponding to fixed bit rate R_2 in the case of pSIC is given by

$$A_2^{pSIC,FD} = \left(1 - OP_2^{pSIC,FD}\right) \times R_2. \tag{37}$$

The sum of the throughput of the system in the case of pSIC at FD mode can be computed by

$$A_{sum}^{pSIC,FD} = \left(1 - OP_1^{FD}\right) \times R_1 + \left(1 - OP_2^{pSIC,FD}\right) \times R_2. \tag{38}$$

In HD mode, throughput performance can be obtained in three cases, as follows

$$A_1^{HD} = \left(1 - OP_1^{HD}\right) \times R_1, \tag{39}$$

$$A_2^{ipSIC,HD} = \left(1 - OP_2^{ipSIC,HD}\right) \times R_2. \tag{40}$$

In the case of ipSIC, the sum throughput of the system can be formulated as

$$A_{sum}^{ipSIC,HD} = \left(1 - OP_1^{HD}\right) \times R_1 + \left(1 - OP_2^{ipSIC,HD}\right) \times R_2, \tag{41}$$

and

$$A_2^{pSIC,HD} = \left(1 - OP_2^{pSIC,HD}\right) \times R_2. \tag{42}$$

In HD mode, the sum throughput of the system in the case of pSIC can be obtained as

$$A_{sum}^{pSIC,HD} = \left(1 - OP_1^{HD}\right) \times R_1 + \left(1 - OP_2^{pSIC,HD}\right) \times R_2. \tag{43}$$

V. APPROXIMATION ANALYSIS

Based on the analytical results in (16), (18), (22), (26), (28) and (31), when $\rho \to \infty$, the asymptotic outage probabilities of the first and second user pairs for ipSIC/pSIC with $e^{-x} \approx 1 - x$ are given as (44)–(47), shown at the bottom of the next page, (48) and (49), as shown at the bottom of the page 10.

In this section, we denote $\tau_2 \triangleq n + m_{h_2}$, $\Xi = \frac{\upsilon_1\gamma_0^2}{\upsilon_2}\left(\frac{\gamma_0^1\upsilon_2}{\upsilon_1\beta_{h_1}}+\frac{1}{\beta_{h_2}}\right)+\frac{1}{\beta_{k_r}}$.

VI. NUMERICAL AND SIMULATION RESULTS

Simulations are accomplished for system performance evaluation in MATLAB to obtain impacts of parameters on FD UL-DL NOMA-assisted UAV system. We provide both analytical and simulation results. The simulation parameters, unless otherwise specified, are $\beta_{h_1} = \left(d_{U_1R}\right)^{-\alpha}, \beta_{h_2} = \left(d_{U_2R}\right)^{-\alpha}, \beta_{g_1} = \left(d_{RU_3}\right)^{-\alpha},$

$$
\begin{aligned}
OP_{1,asym}^{FD} &= 1 - \Pr\left(|h_1|^2 \geq \frac{\gamma_0^1}{\upsilon_1}\left(\upsilon_2|h_2|^2 + |f|^2\right)\right)\left(1 - F_{|g_1|^2}\left(\frac{1}{\upsilon_3 - \upsilon_4\gamma_0^1}\right)\right) \\
&= \sum_{n=0}^{m_{h_1}-1}\sum_{n_1=0}^{n}\binom{n}{n_1}\sum_{n_2=0}^{m_{g_1}-1}\frac{{\upsilon_2}^{n-n_1}}{n!\beta_{h_1}^n}\frac{\Gamma\left(n_1+m_f\right)\Gamma\left(n-n_1+m_{h_2}\right)}{\Gamma\left(m_f\right)\Gamma\left(m_{h_2}\right)\beta_f^{m_f}\beta_{h_2}^{m_{h_2}}} \\
&\quad\times\left(\frac{\gamma_0^1}{\upsilon_1}\right)^n\left(\frac{\gamma_0^1}{\upsilon_1\beta_{h_1}}+\frac{1}{\beta_f}\right)^{-n_1-m_f}\left(\frac{\gamma_0^1\upsilon_2}{\upsilon_1\beta_{h_1}}+\frac{1}{\beta_{h_2}}\right)^{-n+n_1-m_{h_2}} \\
&\quad\times\frac{1}{n_2!\beta_{g_1}^{n_2}}\left(1-\frac{1}{\left(\upsilon_3-\upsilon_4\gamma_0^1\right)\beta_{g_1}}\right)\left(\frac{1}{\upsilon_3-\upsilon_4\gamma_0^1}\right)^{n_2}, \qquad (44)
\end{aligned}
$$

$$
\begin{aligned}
OP_{2,asym}^{ipSIC,FD} &= 1 - \sum_{n=0}^{m_{h_1}-1}\sum_{n_1=0}^{n}\binom{n}{n_1}\sum_{n_2=0}^{\tau_1-1}\sum_{n_3=0}^{n_2}\binom{n_2}{n_3}\frac{{\upsilon_2}^{n-n_1}}{n!\beta_{h_1}^n}\left(\frac{\gamma_0^1}{\upsilon_1}\right)^n \\
&\quad\times\frac{{\upsilon_1}^{n_3}}{n_2!}\left(\frac{\vartheta_1\gamma_0^2}{\upsilon_2}\right)^{n_2}\frac{\left(n-n_1+m_{h_2}-1\right)!{\vartheta_1}^{-\tau_1}}{\Gamma\left(m_{h_2}\right)\beta_{h_2}^{m_{h_2}}\Gamma\left(m_{k_r}\right)\Gamma\left(m_f\right)\beta_{k_r}^{m_{k_r}}\beta_f^{m_f}} \\
&\quad\times\left(\frac{\vartheta_1\gamma_0^2}{\upsilon_2}+\frac{\gamma_0^1}{\upsilon_1\beta_{h_1}}+\frac{1}{\beta_f}\right)^{-n_2+n_3-n_1-m_f}\left(\frac{1}{\beta_{k_r}}+\frac{\vartheta_1\gamma_0^2\upsilon_1}{\upsilon_2}\right)^{-n_3-m_{k_r}} \\
&\quad\times\left(n_2-n_3+n_1+m_f-1\right)!\left(n_3+m_{k_r}-1\right)! \\
&\quad\times\left[\left(1-\frac{1}{\left(\upsilon_3-\upsilon_4\gamma_0^1\right)\beta_{g_2}}\right)\sum_{n_4=0}^{m_{g_2}-1}\frac{1}{n_4!\beta_{g_2}^{n_4}}\left(\frac{1}{\upsilon_3-\upsilon_4\gamma_0^1}\right)^{n_4}\right. \\
&\quad\times\left(1-\frac{1}{\Gamma\left(m_{k_2}\right)}\Gamma\left(m_{k_2},\frac{\upsilon_4}{\gamma_0^1\upsilon_3\beta_{k_2}\left(\upsilon_3-\gamma_0^1\upsilon_4\right)}\right)\right) \\
&\quad\left.+\sum_{n_5=0}^{m_{g_2}-1}\frac{1}{n_5!\beta_{g_2}^{n_5}}\left(\frac{\gamma_0^1\upsilon_3}{\upsilon_4}\right)^{n_5}\left(\frac{\gamma_0^1\upsilon_3}{\upsilon_4\beta_{g_2}}\right)^{-n_5-1}\Gamma\left(n_5+1,\frac{1}{\beta_{g_2}\left(\upsilon_3-\gamma_0^1\upsilon_4\right)}\right)\right], \qquad (45)
\end{aligned}
$$

$$
\begin{aligned}
OP_{2,asym}^{pSIC,FD} &= 1 - \sum_{n=0}^{m_{h_1}-1}\sum_{n_1=0}^{n}\binom{n}{n_1}\sum_{n_2=0}^{\tau_1-1}\sum_{n_3=0}^{n_2}\binom{n_2}{n_3}\sum_{n_4=0}^{m_{g_2}-1}\frac{{\upsilon_2}^{n-n_1}}{n!n_2!\beta_{h_1}^n}\left(\frac{\gamma_0^1}{\upsilon_1}\right)^n\left(\frac{\vartheta_1\gamma_0^2}{\upsilon_2}\right)^{n_2} \\
&\quad\times\frac{{\vartheta_1}^{-\tau_1}\left(n-n_1+m_{h_2}-1\right)!\Gamma\left(n_1+n_3+m_f\right)}{\Gamma\left(m_f\right)\Gamma\left(m_{h_2}\right)\beta_f^{m_f}\beta_{h_2}^{m_{h_2}}}\left(\frac{\gamma_0^1}{\upsilon_1\beta_{h_1}}+\frac{1}{\beta_f}+\frac{\vartheta_1\gamma_0^2}{\upsilon_2}\right)^{-n_1-n_3-m_f} \\
&\quad\times\frac{1}{n_4!\beta_{g_2}^{n_4}}\left(1-\frac{1}{\left(\upsilon_3-\upsilon_4\gamma_0^1\right)\beta_{g_2}}\right)\left(\frac{1}{\upsilon_3-\upsilon_4\gamma_0^1}\right)^{n_4}, \qquad (46)
\end{aligned}
$$

$$
\begin{aligned}
OP_{1,asym}^{HD} &= 1 - \Pr\left(|h_1|^2 \geq \frac{\upsilon_2\gamma_0^1}{\upsilon_1}|h_2|^2\right)\left(1 - F_{|g_1|^2}\left(\frac{1}{\upsilon_3-\upsilon_4\gamma_0^1}\right)\right) \\
&= \sum_{n=0}^{m_{h_1}-1}\sum_{n_1=0}^{m_{g_1}-1}\frac{\Gamma\left(n+m_{h_2}\right)}{n!n_1!\Gamma\left(m_{h_2}\right)\beta_{h_1}^n\beta_{g_1}^{n_1}\beta_{h_2}^{m_{h_2}}}\left(\frac{\upsilon_2\gamma_0^1}{\upsilon_1}\right)^n \\
&\quad\times\left(1-\frac{1}{\left(\upsilon_3-\upsilon_4\gamma_0^1\right)\beta_{g_1}}\right)\left(\frac{1}{\upsilon_3-\upsilon_4\gamma_0^1}\right)^{n_1}\left(\frac{\gamma_0^1\upsilon_2}{\upsilon_1\beta_{h_1}}+\frac{1}{\beta_{h_2}}\right)^{-n-m_{h_2}} \qquad (47)
\end{aligned}
$$

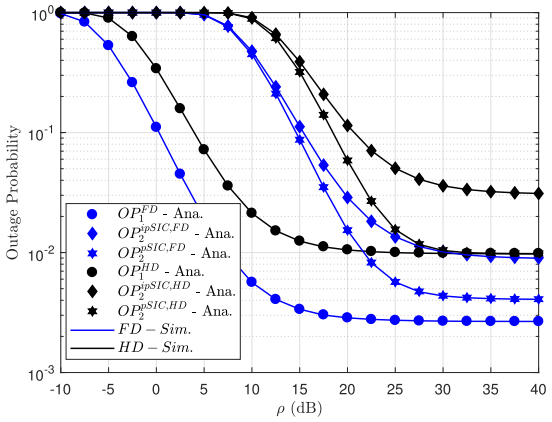

FIGURE 2. Outage probability comparison of first and second user pairs related to FD-NOMA /HD-NOMA, and impact of ipSIC /pSIC.

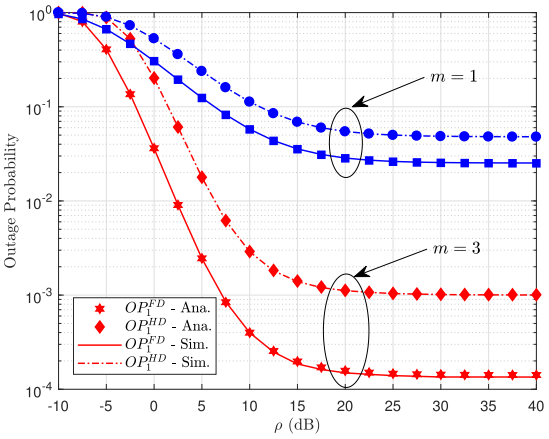

FIGURE 3. Comparison of outage probability of first user pair between cooperative FD-NOMA /HD-NOMA with different values of *m*.

$\beta_{g_2} = \left(d_{RU_4}\right)^{-\alpha}$, $\beta_{k_r} = \kappa\beta_{h_1}$, $\beta_{k_2} = \kappa\beta_{g_2}$ with $\kappa = 0.003$; $x_{U_1} = 2, x_{U_2} = 5, x_{U_3} = 5, x_{U_4} = 2$; $r = 0.5$; $\Phi = \pi$; $h = 1$; path loss exponent $\alpha = 0.5$. For the sake of comparison, simulation results of HD-NOMA and HD-OMA are also presented. The proportional fairness criteria [29], i.e., equal transmission power ($P_1 = P_2 = 0.5$) and equal bandwidth ($\beta_w = 0.5$) allocated to each user, are considered for HD-OMA. The strict match curves between the analytical and simulation results confirms the correctness of the authors analysis presented here. For the sake of comparison, simulation results of HD-NOMA scenarios is also presented as a benchmark. Some related parameters are provided in Table 1.

In Fig. 2, outage performance comparison between HD-NOMA and FD-NOMA is presented under ipSIC/pSIC with Nakagami-*m* fading parameter set $m = 2$. In this figure, it can be seen that FD-NOMA has significantly better outage performance than that of HD-NOMA, for each case. From this illustration, it can also be observed that outage performance of these cases decreases linearly in the low-to-moderate SNR regime, but saturates in the high SNR regime. Interference exists due to the mode of ipSIC, which is the main reason for the occurrence of the performance gap between pSIC and ipSIC in each mode (i.e. HD and FD).

Fig. 3 shows the performance of outage probability of NOMA for the first user pair in a comparison of FD and HD modes under two different fading parameters: $m = 1, m = 3$. It can be observed that the larger the fading parameters are,

$$
\begin{aligned}
OP_{2,asym}^{ipSIC,HD} = 1 - &\sum_{n=0}^{m_{h_1}-1}\sum_{n_1=0}^{\tau_2-1}\frac{(n+m_{h_2}-1)!\,(n_1+m_{k_r}-1)!\,\Xi^{-n_1-m_{k_r}}}{n!n_1!\Gamma\left(m_{h_2}\right)\Gamma\left(m_{k_r}\right)\beta_{k_r}^{m_{k_r}}\beta_{h_1}^{n}\beta_{h_2}^{m_{h_2}}}\\
&\times\left(\frac{\upsilon_2\gamma_0^1}{\upsilon_1}\right)^{n}\left(\frac{\upsilon_1\gamma_0^2}{\upsilon_2}\right)^{n_1}\left(\frac{\gamma_0^1\upsilon_2}{\upsilon_1\beta_{h_1}}+\frac{1}{\beta_{h_2}}\right)^{-n-m_{h_2}+n_1}\\
&\times\Bigg[\left(1-\frac{1}{\left(\upsilon_3-\upsilon_4\gamma_0^1\right)\beta_{g_2}}\right)\sum_{n_2=0}^{m_{g_2}-1}\frac{1}{n_2!\beta_{g_2}^{n_2}}\left(\frac{1}{\upsilon_3-\upsilon_4\gamma_0^1}\right)^{n_2}\\
&\times\left(1-\frac{1}{\Gamma\left(m_{k_2}\right)}\Gamma\left(m_{k_2},\frac{\upsilon_4}{\gamma_0^1\upsilon_3\beta_{k_2}\left(\upsilon_3-\gamma_0^1\upsilon_4\right)}\right)\right)\\
&+\sum_{n_3=0}^{m_{g_2}-1}\frac{1}{n_3!\beta_{g_2}^{n_3}}\left(\frac{\gamma_0^1\upsilon_3}{\upsilon_4}\right)^{n_3}\left(\frac{\gamma_0^1\upsilon_3}{\upsilon_4\beta_{g_2}}\right)^{-n_3-1}\Gamma\left(n_3+1,\frac{1}{\beta_{g_2}\left(\upsilon_3-\gamma_0^1\upsilon_4\right)}\right)\Bigg],
\end{aligned}
\tag{48}
$$

$$
\begin{aligned}
OP_{2,asym}^{pSIC,HD} = 1 - &\sum_{n=0}^{m_{h_1}-1}\frac{\left(\upsilon_2\gamma_0^1/\upsilon_1\right)^{n}\Gamma\left(n+m_{h_2},\Xi_1\right)}{n!\Gamma\left(m_{h_2}\right)\beta_{h_1}^{n}\beta_{h_2}^{m_{h_2}}}\left(\frac{\upsilon_2\gamma_0^1}{\upsilon_1\beta_{h_1}}+\frac{1}{\beta_{h_2}}\right)^{-n-m_{h_2}}\\
&\times\left(1-\frac{1}{\left(\upsilon_3-\upsilon_4\gamma_0^1\right)\beta_{g_2}}\right)\sum_{n_1=0}^{m_{g_2}-1}\frac{1}{n_1!\beta_{g_2}^{n_1}}\left(\frac{1}{\upsilon_3-\upsilon_4\gamma_0^1}\right)^{n_1}
\end{aligned}
\tag{49}
$$

TABLE 1. All parameters in the related simulations.

–	*Rate*	β_f	Power allocation factors	κ	ρ	α	m
Figure 2	$R_1 = 0.1, R_2 = 0.5$	0.01	$v_1 = 0.6, v_2 = 0.4, v_3 = 0.7, v_4 = 0.3$	0.01	–	0.5	2
Figure 3	$R_1 = 0.1, R_2 = 0.5$	0.01	$v_1 = 0.6, v_2 = 0.4, v_3 = 0.7, v_4 = 0.3$	0.01	–	0.5	1, 3
Figure 4	$R_1 = 0.1, R_2 = 0.5$	0.01	$v_1 = 0.6, v_2 = 0.4, v_3 = 0.7, v_4 = 0.3$	0.01	–	0.5	1, 3
Figure 5	$R_1 = 0.1, R_2 = 0.5$	0.01	$v_1 = 0.6, v_2 = 0.4, v_3 = 0.7, v_4 = 0.3$	0.01	10, 40	0.5	3
Figure 6	$R_1 = 0.1, R_2 = 0.5$	–	$v_1 = 0.6, v_2 = 0.4, v_3 = 0.7, v_4 = 0.3$	0.03	10, 40	0.1	3
Figure 7	$R_1 = 0.1, R_2 = 0.5$	0.01	$v_1 = 0.6, v_2 = 0.4, v_3 = 0.7, v_4 = 0.3$	0.1	–	0.5	4
Figure 8	$R_1 = 0.1$	0.01	$v_1 = 0.6, v_2 = 0.4, v_3 = 0.7, v_4 = 0.3$	0.1	10, 40	0.5	3
Figure 9	–	0.1	$v_1 = 0.6, v_2 = 0.4, v_3 = 0.7, v_4 = 0.3$	0.1	40	0.1	2
Figure 10	$R_1 = 0.1, R_2 = 0.5$	0.01	$v_1 = 0.6, v_2 = 0.4, v_3 = 0.9, v_4 = 0.1$	0.1	–	0.5	4
Figure 11	$R_1 = 0.1, R_2 = 0.5$	0.03	$v_1 = 0.9, v_2 = 0.1, v_3 = 0.6, v_4 = 0.4$	0.1	–	0.5	2
Figure 12	$R_1 = 0.1, R_2 = 0.5$	0.03	$v_1 = 0.6, v_2 = 0.4, v_3 = 0.9, v_4 = 0.1$	0.1	–	0.5	2
Figure 13	$R_1 = 0.5, R_2 = 0.5$	0.003	$v_1 = 0.65, v_2 = 0.35, v_3 = 0.9, v_4 = 0.1$	0.02^3	–	4	–
Figure 14	$R_1 = 0.5, R_2 = 0.5$	0.003	$v_1 = 0.65, v_2 = 0.35, v_3 = 0.9, v_4 = 0.1$	0.02^3	–	4	–

the better outage performance NOMA exhibits. The main reason for this is that a larger fading parameter leads to a higher diversity order for the user, and hence a lower outage probability. Specially, these Nakagami channels become Rayleigh fading when $m = 1$; this situation is known as the worst outage performance. In the case of the second user pair, a similar observation can be obtained, as shown in Fig. 4. In this scenario, the pSIC case outperforms the ipSIC case. The lower performance is the resulted of the existence of residual self-interference due to ipSIC. Intuitively, the increase of fading parameters m dramatically decreases the concerned probabilities. It can be explained that the existence of line of sight (LoS) for a user with higher channel gain can dramatically decrease the outage probability.

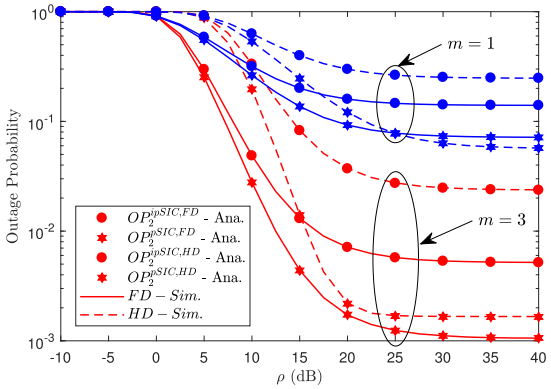

FIGURE 4. Comparison of outage probability of second user pair in FD-NOMA /HD-NOMA under impact of ipSIC and pSIC with different values of *m*.

Fig. 5 shows that outage performance will be worse at high levels of interference due to the ipSIC case under the different given SNRs. It can be seen that higher SNR brings lower outage performance. In these curves, FD performance is still better than in the HD case. At approximately $\kappa = -5\,(dB)$, the considered NOMA system stops its transmission, what is important to maintain a small enough level of interference related SIC. The main reason for this is that higher κ causes increased interference in the denominator value of the

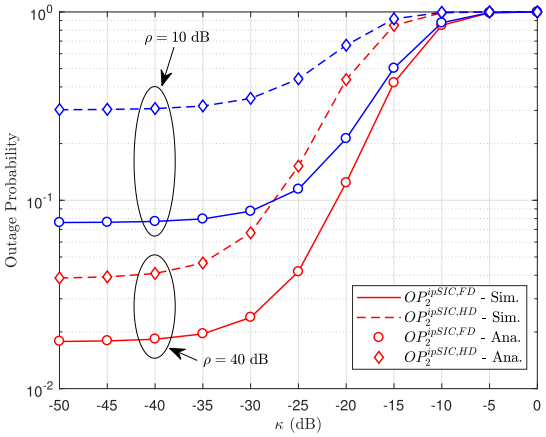

FIGURE 5. Outage probability comparison of second user pair between cooperative FD-NOMA /HD-NOMA under impact of two values of κ.

expression to calculate SINR, which situation leads to outage behavior.

Fig. 6 shows the outage probability of two user pairs at different transmit SNRs with respect to how strong the self-interference channel is. This self-interference channel is strong due to FD mode, and so outage performance will

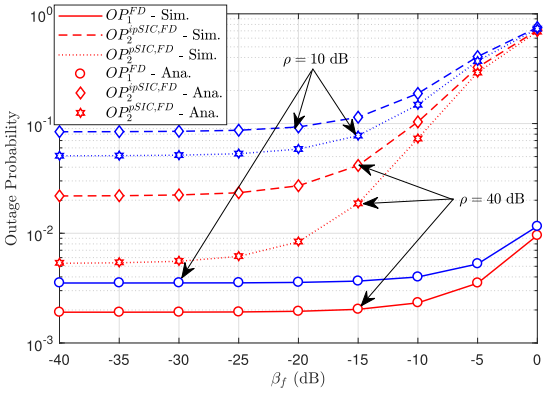

FIGURE 6. Outage probability comparison of two cases of FD-NOMA under impact of ipSIC/pSIC different values of β_f.

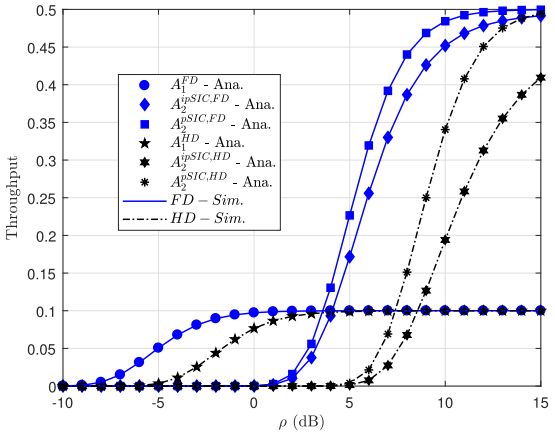

FIGURE 7. Throughput performance analysis.

be worse. It can be seen that when β_f is in a low range, i.e. -40 (dB) to -25 (dB), stable outage level is maintained.

Fig. 7 illustrates throughput versus transmit SNR ρ. It can be clearly seen that NOMA with pSIC in FD mode exhibits the highest performance. The first user pair achieves throughput performance lower than that of the second user pair when SIC is employed. The main reason is that different power allocation factors result in throughput performance gaps. In this case, FD mode is better than HD mode in all related cases. In a high SNR regime, high SNR contributes to throughput behavior more strongly than do the remaining parameters, i.e. parameters that belong to imperfect/pSIC, and hence the same throughput value can occur at very high SNR.

Fig. 8 shows impacts of target rate R_2 on outage performance in several situations of HD/FD and ipSIC/pSIC. The interesting point is that higher target rate leads to worse outage performance. According to this observation, our system meets an outage event at $R_2 = 4(bps/Hz)$ except for NOMA with ipSIC in FD mode. For an overall evaluation of the two target rates, i.e. R_1, R_2, we further simulate the outage performance, with results shown in Fig. VI. It can be shown

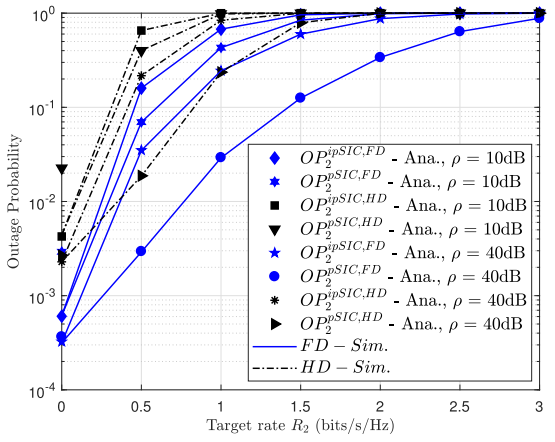

FIGURE 8. Outage probability comparison of second user pair in FD-NOMA/HD-NOMA under impact of ipSIC and pSIC with different of R_2.

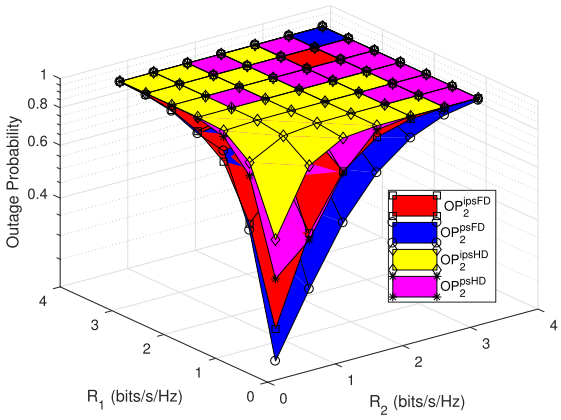

FIGURE 9. Outage probability comparison of second user pair in FD-NOMA/HD-NOMA under impact of ipSIC and pSIC with different data rates of R_1 and R_2.

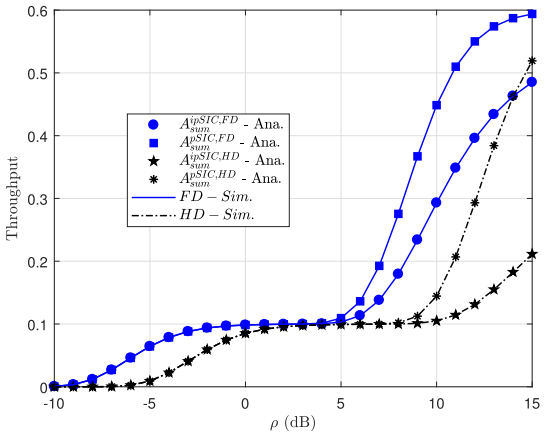

FIGURE 10. Sum throughput of system in FD-NOMA/HD-NOMA under impact of ipSIC and pSIC.

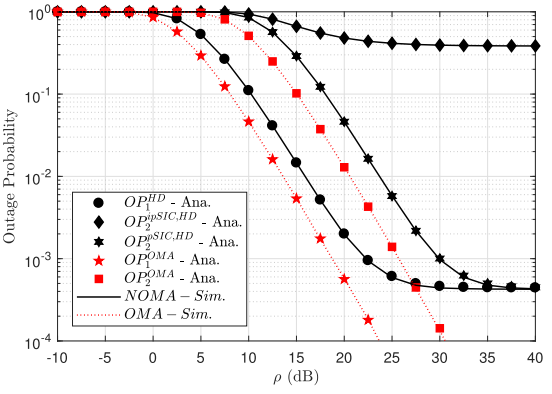

FIGURE 11. Outage probability comparison of second user pair in NOMA with OMA.

that the best outage performance occurs when the lowest data rates are employed.

Fig. 10 provides further information on sum throughput of FD-NOMA and HD-NOMA. It can be seen clearly that the pSIC case exhibits higher throughput at high ρ. This situation

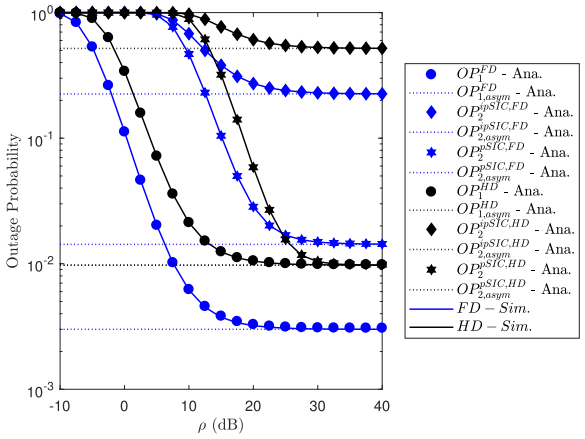

FIGURE 12. Comparison of asymptotic outage probability of the first user pair between cooperative FD-NOMA /HD-NOMA.

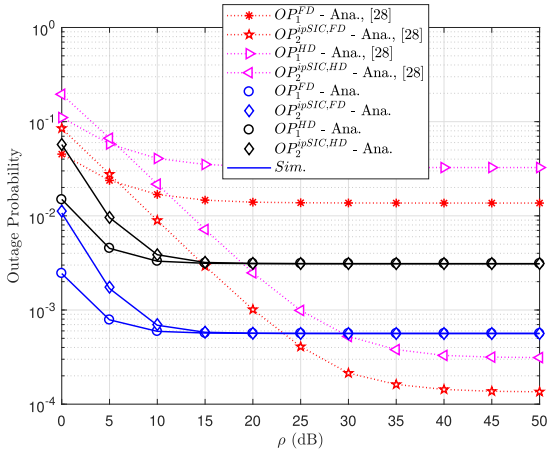

FIGURE 13. Comparison of outage probability of two user pairs between cooperative FD-NOMA /HD-NOMA under impact of ipSIC with result reported in [28].

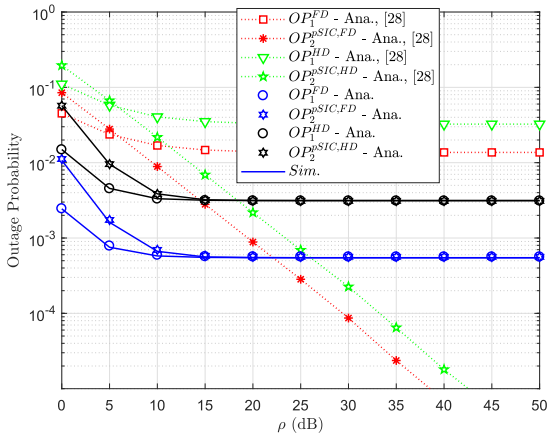

FIGURE 14. Comparison of outage probability of two user pairs between cooperative FD-NOMA /HD-NOMA (pSIC) with result reported in [28].

matches previous simulation results. Fig. 11 confirms that outage performance in the OMA case is better than that of NOMA. The main reason for this is that the power splitting factor allocated to the two NOMA signals results in worse outage behavior in the case of NOMA. Other trends can be seen to be similar to those of previous experiments. Fig. 12 show the lower bound of outage performance for every considered case.

In Fig. 13, we compare our results with the work [28] in the case of ipSIC. It is necessary to change our previous parameters to consistent with that in [28]. In particular, the outage performance of the first user pair with both FD and HD modes in our paper is better than that in [28] in entire range of ρ. While considering the second user pair with FD mode in our result only outperforms that that in [28] at the range of ρ from 0 to 23 dB. Similar trend of the second user pair can be seen clearly in HD mode, but our result exhibits better performance at the range of ρ from 0 to 30 dB. In Fig. 14, similar comparison can be achieved for our paper and the work in [28] in the case of pSIC.

VII. CONCLUSION

In this investigation, a novel NOMA-based uplink/downlink UAV system has been suggested that considers impacts of main factors such as different fading parameters of the Nakagami-m channel. Specifically, by employing FD at the UAV and SIC technique at the receivers, system benefits from the ability of the UAV as a relay to serve two user pairs simultaneously, without requirement of extra bandwidth. On the other hand, the limitation of self-interference due to FD mode provides reasonable outage and throughput performance. These metrics lead to improve data transmission efficiency. This is certainly an important achievement in that we have analyzed the performance of the considered system serving two pairs of users and derived closed-form expressions for the outage probability of each user pair. The theoretical derivations were confirmed and are in strict agreement with the simulation results. Our future concern will be enhancement design of NOMA-assisted UAV system to serve multiple pairs of users.

APPENDIX A
PROOF OF PROPOSITION 1

By implementing order statistics of separated components, OP_1^{FD} can be obtained

$$OP_1^{FD} = 1 - \underbrace{\left(1 - F_{|h_1|^2}\left(\frac{\gamma_0^1}{\upsilon_1 \rho_S}\left(\upsilon_2 \rho_S |h_2|^2 + \rho_R |f|^2 + 1\right)\right)\right)}_{\varpi_1} \times \underbrace{\left(1 - F_{|g_1|^2}\left(\frac{\gamma_0^1}{\left(\upsilon_3 - \upsilon_4 \gamma_0^1\right)\rho_R}\right)\right)}_{\varpi_2}. \quad \text{(A.1)}$$

To address final outage event, we computed these outage expressions as follows

$$\varpi_1 = 1 - F_{|h_1|^2}\left(\frac{\gamma_0^1}{\upsilon_1 \rho_S}\left(\upsilon_2 \rho_S |h_2|^2 + \rho_R |f|^2 + 1\right)\right)$$

$$= \int_0^{\infty} \varpi_1(x,y) f_y(y)\, dy \int_0^{\infty} f_x(x)\, dx. \quad \text{(A.2)}$$

After the implementation of the calculation, we have

$$\varpi_1(x,y) = e^{-\frac{\gamma_0^1}{\upsilon_1\rho_S\beta_{h_1}}} \sum_{n=0}^{m_{h_1}-1} \sum_{n_1=0}^{n} \sum_{n_2=0}^{n_1} \binom{n}{n_1}\binom{n_1}{n_2} \times \frac{1}{n!\beta_{h_1}^n}\left(\frac{\gamma_0^1}{\upsilon_1\rho_S}\right)^n \rho_R^{n_2}(\upsilon_2\rho_s)^{n_1-n_2} \times e^{-\frac{\gamma_0^1\rho_r x}{\upsilon_1\rho_S\beta_{h_1}}} x^{n_2} e^{-\frac{\gamma_0^1\upsilon_2 y}{\upsilon_1\beta_{h_1}}} y^{n_1-n_2}. \quad \text{(A.3)}$$

To further computation, we have

$$\begin{aligned}\varpi_1 &= e^{-\frac{\gamma_0^1}{\upsilon_1\rho_S\beta_{h_1}}} \sum_{n=0}^{m_{h_1}-1} \sum_{n_1=0}^{n} \sum_{n_2=0}^{n_1} \binom{n}{n_1}\binom{n_1}{n_2} \times \frac{1}{n!\beta_{h_1}^n}\left(\frac{\gamma_0^1}{\upsilon_1\rho_S}\right)^n (\rho_R)^{n_2}(\upsilon_2\rho_S)^{n_1-n_2} \times \int_0^{\infty} e^{-\frac{\gamma_0^1\upsilon_2 y}{\upsilon_1\beta_{h_1}}} y^{n_1-n_2} f_{|h_2|^2}(y)dy \times \int_0^{\infty} e^{-\frac{\gamma_0^1\rho_R x}{\upsilon_1\rho_S\beta_{h_1}}} x^{n_2} f_{|f|^2}(x)dx \\ &= e^{-\frac{\gamma_0^1}{\upsilon_1\rho_S\beta_{h_1}}} \sum_{n=0}^{m_{h_1}-1} \sum_{n_1=0}^{n} \sum_{n_2=0}^{n_1} \binom{n}{n_1}\binom{n_1}{n_2} \frac{1}{n!\beta_{h_1}^n} \times \left(\frac{\gamma_0^1}{\upsilon_1\rho_S}\right)^n \frac{1}{\Gamma(m_f)\beta_f^{m_f}} \left(\frac{\gamma_0^1\rho_R}{\upsilon_1\rho_S\beta_{h_1}} + \frac{1}{\beta_f}\right)^{-n_2-m_f} \times \Gamma(n_2+m_f)\Gamma(n_1-n_2+m_{h_2})\rho_r^{n_2}(\upsilon_2\rho_S)^{n_1-n_2} \times \frac{1}{\Gamma(m_{h_2})\beta_{h_2}^{m_{h_2}}} \left(\frac{\gamma_0^1\upsilon_2}{\upsilon_1\beta_{h_1}} + \frac{1}{\beta_{h_2}}\right)^{-n_1+n_2-m_{h_2}}, \quad \text{(A.4)}\end{aligned}$$

and

$$\varpi_2 = 1 - F_{|g_1|^2}\left(\frac{\gamma_0^1}{(\upsilon_3-\upsilon_4\gamma_0^1)\rho_R}\right) = \sum_{n_3=0}^{m_{g_1}-1} \frac{e^{-\frac{\gamma_0^1}{(\upsilon_3-\upsilon_4\gamma_0^1)\rho_R\beta_{g_1}}}}{n_3!\beta_{g_1}^{n_3}} \left(\frac{\gamma_0^1}{(\upsilon_3-\upsilon_4\gamma_0^1)\rho_R}\right)^{n_3}. \quad \text{(A.5)}$$

Plugging above values of (A.4) and (A.5) into (A.1) we obtain the final formula.

This is end of proof.

APPENDIX B
PROOF OF PROPOSITION 2

After simple manipulations, we have following equation as

$$\Psi_1 = \Pr\left(\gamma_{R\leftarrow 1} \geq \gamma_0^1, \gamma_{R\leftarrow 2}^{ipSIC} \geq \gamma_0^2\right) = \Pr\left(\begin{array}{c}\frac{\upsilon_1\rho_S|h_1|^2}{\upsilon_2\rho_S|h_2|^2+\rho_R|f|^2+1} \geq \gamma_0^1, \\ \frac{\upsilon_2\rho_S|h_2|^2}{\upsilon_1\rho_S|k_r|^2+\rho_R|f|^2+1} \geq \gamma_0^2\end{array}\right). \quad \text{(B.1)}$$

After placing the following variables $x = |f|^2$, $y = |h_2|^2$, $z = |k_r|^2$ and performing calculations, we have

$$\Psi_1 = \int_{\frac{\gamma_0^2}{\upsilon_2\rho_S}(\upsilon_1\rho_S z+\rho_R x+1)}^{\infty} \Omega_1(x,y) f_y(y)\, dy \times \int_0^{\infty} f_x(x)\, dx \int_0^{\infty} f_z(z)\, dz, \quad \text{(B.2)}$$

with

$$\begin{aligned}\Omega_1(x,y) &= 1 - F_{|h_1|^2}\left(\frac{\gamma_0^1}{\upsilon_1\rho_S}(\upsilon_2\rho_S y + \rho_R x + 1)\right) \\ &= e^{-\frac{\gamma_0^1(\upsilon_2\rho_S y+\rho_R x+1)}{\upsilon_1\rho_S\beta_{h_1}}} \times \sum_{n=0}^{m_{h_1}-1} \sum_{n_1=0}^{n} \sum_{n_2=0}^{n_1} \binom{n}{n_1}\binom{n_1}{n_2} \times \left(\frac{\gamma_0^1}{\upsilon_1}\right)^n \frac{\rho_R^{n_2}\upsilon_2^{n_1-n_2}}{n!\beta_{h_1}^n\rho_S^{n-n_1+n_2}} x^{n_2} y^{n_1-n_2}. \quad \text{(B.3)}\end{aligned}$$

It is noted that the last step can be achieved by using trinomial expansion [[34], eq. (1.111)]. Plugging (B.3) in (B.2), after some manipulatons with the help of [[34], eq. (3.381.3), eq. (3.381.4) and eq. (8.352.2)], we have

$$\begin{aligned}\Psi_1 = &\sum_{n=0}^{m_{h_1}-1} \sum_{n_1=0}^{n} \sum_{n_2=0}^{n_1} \binom{n}{n_1}\binom{n_1}{n_2} \times \frac{\rho_R^{n_2}\upsilon_2^{n_1-n_2}e^{-\frac{\gamma_0^1}{\upsilon_1\rho_S\beta_{h_1}}}}{n!\beta_{h_1}^n\rho_S^{n-n_1+n_2}} \left(\frac{\gamma_0^1}{\upsilon_1\rho_S}\right)^n \times \int_0^{\infty} \Omega_2(x,z)\, e^{-x\left(\frac{\gamma_0^1\rho_R}{\upsilon_1\rho_S\beta_{h_1}}+\frac{1}{\beta_f}\right)} x^{n_2+m_f-1} dx \times \frac{1}{\Gamma(m_{k_r})\Gamma(m_f)\beta_{k_r}^{m_{k_r}}\beta_f^{m_f}} \int_0^{\infty} z^{m_{k_r}-1} e^{-\frac{z}{\beta_{k_r}}} dz, \end{aligned} \quad \text{(B.4)}$$

with

$$\Omega_2(x,z) = \int_{\frac{\gamma_0^2}{\upsilon_2\rho_S}(\upsilon_1\rho_S z+\rho_R x+1)}^{\infty} e^{-\frac{\gamma_0^1\upsilon_2 y}{\upsilon_1\beta_{h_1}}} y^{n_1-n_2} f_y(y)\, dy = \frac{\Gamma(\tau_1)\vartheta_1^{-\tau_1}}{\Gamma(m_{h_2})\beta_{h_2}^{m_{h_2}}} e^{-\frac{\vartheta_1\gamma_0^2}{\upsilon_2\rho_S}}$$

$$\times \sum_{n_3=0}^{\tau_1-1} \sum_{n_4=0}^{n_3} \sum_{n_5=0}^{n_4} \binom{n_3}{n_4} \binom{n_4}{n_5} \frac{1}{n_3!} \times {\rho_R}^{n_4-n_5} {\upsilon_1}^{n_5} {\rho_S}^{n_5} \left(\frac{\vartheta_1 \gamma_0^2}{\upsilon_2 \rho_S}\right)^{n_3} \times e^{-\frac{\vartheta_1 \gamma_0^2 \rho_R x}{\upsilon_2 \rho_S}} x^{n_4-n_5} e^{-\frac{\vartheta_1 \gamma_0^2 \upsilon_1 z}{\upsilon_2}} z^{n_5}, \tag{B.5}$$

where $\tau_1 \triangleq n_1 - n_2 + m_{h_2}$ and $\vartheta_1 \triangleq \frac{\gamma_0^1 \upsilon_2}{\upsilon_1 \beta_{h_1}} + \frac{1}{\beta_{h_2}}$. Finally, replacing (B.5)) into (B.4), we obtain final formula of Ψ_1.

To achieve Ψ_2, we have

$$\begin{aligned}\Psi_2 &= \Pr\left(\gamma_{U_4 \leftarrow 1} \geq \gamma_0^1, \gamma_{U_4}^{ipSIC} \geq \gamma_0^2\right) \\ &= \Pr\left(\frac{\upsilon_3 \rho_R |g_2|^2}{\upsilon_4 \rho_R |g_2|^2 + 1} \geq \gamma_0^1, \frac{\upsilon_4 \rho_R |g_2|^2}{\upsilon_3 \rho_R |k_2|^2 + 1} \geq \gamma_0^2\right).\end{aligned} \tag{B.6}$$

Putting $\vartheta_2 \triangleq \max\left(0, \frac{1}{\upsilon_3 \rho_R}\left(\frac{\upsilon_4 \gamma_0^1}{(\upsilon_3 - \gamma_0^1 \upsilon_4)\gamma_0^2} - 1\right)\right)$, ϑ_2 can be given as

$$\begin{aligned}\Psi_2 &= \Pr\left(|g_2|^2 \geq \max\left(\frac{\gamma_0^1}{(\upsilon_3 - \gamma_0^1 \upsilon_4)\rho_r}, \frac{\gamma_0^2}{\upsilon_4 \rho_R}\left(\upsilon_3 \rho_R |k_2|^2 + 1\right)\right)\right) \\ &= \underbrace{\Pr\left(|g_2|^2 \geq \frac{\gamma_0^2}{\upsilon_4 \rho_R}\left(\upsilon_3 \rho_R |k_2|^2 + 1\right), |k_2|^2 > \vartheta_2\right)}_{\triangleq \xi_1} \\ &\quad + \underbrace{\Pr\left(|g_2|^2 \geq \frac{\gamma_0^1}{\left(\upsilon_3 - \gamma_0^1 \upsilon_4\right)\rho_R}, |k_2|^2 \leq \vartheta_2\right)}_{\triangleq \xi_2},\end{aligned} \tag{B.7}$$

It can be shown that

$$\begin{aligned}\xi_1 &= \int_{\vartheta}^{\infty} \left(1 - F_{|g_2|^2}\left(\frac{\gamma_0^2}{\upsilon_4 \rho_R}\left(\upsilon_3 \rho_R x + 1\right)\right)\right) f_{|k_2|^2}(x)\, dx \\ &= e^{-\frac{\gamma_0^2}{\upsilon_4 \rho_R \beta_{g_2}}} \sum_{n_6=0}^{m_{g_2}-1} \sum_{n_7=0}^{n_6} \binom{n_6}{n_7} \frac{{\upsilon_3}^{n_7} {\rho_R}^{n_7}}{n_6! \beta_{g_2}^{n_6}} \left(\frac{\gamma_0^2}{\upsilon_4 \rho_R}\right)^{n_6} \\ &\quad \times \frac{1}{\Gamma\left(m_{k_2}\right) \beta_{k_2}^{m_{k_2}}} \int_{\vartheta}^{\infty} e^{-x\left(\frac{\gamma_0^2 \upsilon_3}{\upsilon_4 \beta_{g_2}} + \frac{1}{\beta_{k_2}}\right)} x^{n_7 + m_{k_2} - 1} dx.\end{aligned} \tag{B.8}$$

Finally, by using the last equation follows the fact that $\int_u^{\infty} x^{v-1} e^{-\mu x} dx = \mu^{-v} \Gamma(v, \mu u)$ in [30, eq. (3.381.3)] we can obtain

$$\begin{aligned}\xi_1 &= e^{-\frac{\gamma_0^2}{\upsilon_4 \rho_R \beta_{g_2}}} \sum_{n_6=0}^{m_{g_2}-1} \sum_{n_7=0}^{n_6} \binom{n_6}{n_7} \frac{{\upsilon_3}^{n_7} {\rho_R}^{n_7}}{n_6! \beta_{g_2}^{n_6}} \\ &\quad \times \frac{1}{\Gamma\left(m_{k_2}\right) \beta_{k_2}^{m_{k_2}}} \left(\frac{\gamma_0^2 \upsilon_3}{\upsilon_4 \beta_{g_2}} + \frac{1}{\beta_{k_2}}\right)^{-n_7 - m_{k_2}} \\ &\quad \times \left(\frac{\gamma_0^2}{\upsilon_4 \rho_R}\right)^{n_6} \Gamma\left(n_7 + m_{k_2}, \left(\frac{\vartheta_2 \gamma_0^2 \upsilon_3}{\upsilon_4 \beta_{g_2}} + \frac{\vartheta_2}{\beta_{k_2}}\right)\right),\end{aligned} \tag{B.9}$$

and

$$\begin{aligned}\xi_2 &= \left(1 - F_{|g_2|^2}\left(\frac{\gamma_0^1}{\left(\upsilon_3 - \gamma_0^1 \upsilon_4\right)\rho_R}\right)\right) \times F_{|k_2|^2}(\vartheta_2) \\ &= \frac{1}{\Gamma\left(m_{g_2}\right)} \Gamma\left(m_{g_2}, \frac{\gamma_0^1}{\left(\upsilon_3 - \gamma_0^1 \upsilon_4\right)\rho_R \beta_{g_2}}\right) \\ &\quad \times \left(1 - \frac{1}{\Gamma\left(m_{k_2}\right)} \Gamma\left(m_{k_2}, \frac{\vartheta_2}{\beta_{k_2}}\right)\right).\end{aligned} \tag{B.10}$$

Substituting (B.9)) and (B.10) into (B.7), we obtain the final formula of Ψ_2.

It completes the proof.

APPENDIX C
PROOF OF PROPOSITION 3

Similar with steps in Proof of Position 2, Ψ_3 can be calculated as (C.1), shown at the bottom of the next page. While Ψ_4 can be computed as

$$\begin{aligned}&\Psi_4 \\ &= \Pr\left(\gamma_{U_4 \leftarrow 1} \geq \gamma_0^1, \gamma_{U_4}^{pSIC} \geq \gamma_0^2\right) \\ &= \Pr\left(\frac{\upsilon_3 \rho_r |g_2|^2}{\upsilon_4 \rho_R |g_2|^2 + 1} \geq \gamma_0^1, \upsilon_4 \rho_R |g_2|^2 \geq \gamma_0^2\right) \\ &= \Pr\left(|g_2|^2 \geq \max\left(\frac{\gamma_0^1}{\upsilon_3 \rho_R - \gamma_0^1 \upsilon_4 \rho_R}, \frac{\gamma_0^2}{\upsilon_4 \rho_R}\right)\right) \\ &= \frac{1}{\Gamma\left(m_{g_2}\right)} \Gamma\left(m_{g_2}, \frac{1}{\beta_{g_2}} \max\left(\frac{\gamma_0^1}{\upsilon_3 \rho_R - \gamma_0^1 \upsilon_4 \rho_R}, \frac{\gamma_0^2}{\upsilon_4 \rho_R}\right)\right).\end{aligned} \tag{C.2}$$

It completes the proof.

APPENDIX D
PROOF OF PROPOSITION 4

By implementing order statistics of separated components, OP_1^{HD} can be obtained

$$\begin{aligned}OP_1^{HD} &= 1 - \underbrace{\Pr\left(|h_1|^2 \geq \frac{\gamma_{0,HD}^1}{\upsilon_1 \rho_S}\left(\upsilon_2 \rho_S |h_2|^2 + 1\right)\right)}_{\triangleq \varpi_3} \\ &\quad \times \underbrace{\left(1 - F_{|g_1|^2}\left(\frac{\gamma_{0,HD}^1}{\left(\upsilon_3 - \upsilon_4 \gamma_{0,HD}^1\right)\rho_R}\right)\right)}_{\triangleq \varpi_4}.\end{aligned} \tag{D.1}$$

To address final outage event, it need be computed these outage expressions as follows

$$\varpi_3 = E_{|h_1|^2}\left\{1 - F_{|h_1|^2}\left(\frac{\gamma^1_{0,HD}}{\upsilon_1\rho_S}\left(\upsilon_2\rho_S|h_2|^2+1\right)\right)\right\}, \tag{D.2}$$

where $E\{.\}$ indicates the expectation operator. After the implementation of the calculation, we have

$$\begin{aligned}&\varpi_3(y)\\ &= e^{-\frac{\gamma^1_{0,HD}}{\upsilon_1\rho_S\beta_{h_1}}} e^{-\frac{\gamma^1_{0,HD}\upsilon_2\rho_S y}{\upsilon_1\rho_S\beta_{h_1}}}\\ &\quad\times\sum_{n=0}^{m_{h_1}-1}\sum_{n_1=0}^{n}\binom{n}{n_1}\frac{1}{n!}\left(\frac{\gamma^1_{0,HD}}{\upsilon_1\rho_S\beta_{h_1}}\right)^n \upsilon_2^{n_1}\rho_S^{n_1}y^{n_1}.\end{aligned} \tag{D.3}$$

Then, we have following result as

$$\begin{aligned}&\varpi_3\\ &= e^{-\frac{\gamma^1_{0,HD}}{\upsilon_1\rho_S\beta_{h_1}}}\sum_{n=0}^{m_{h_1}-1}\sum_{n_1=0}^{n}\binom{n}{n_1}\frac{1}{n!}\left(\frac{\gamma^1_{0,HD}}{\upsilon_1\rho_S\beta_{h_1}}\right)^n\\ &\quad\times\frac{\upsilon_2^{n_1}\rho_S^{n_1}\Gamma\left(n_1+m_{h_2}\right)}{\Gamma\left(m_{h_2}\right)\beta_{h_2}^{m_{h_2}}}\left(\frac{\gamma^1_{0,HD}\upsilon_2}{\upsilon_1\beta_{h_1}}+\frac{1}{\beta_{h_2}}\right)^{-n_1-m_{h_2}},\end{aligned} \tag{D.4}$$

and

$$\begin{aligned}\varpi_4 &= F_{|g_1|^2}\left(\frac{\gamma^1_{0,HD}}{\left(\upsilon_3-\upsilon_4\gamma^1_0\right)\rho_R}\right)\\ &= 1-e^{-\frac{\gamma^1_{0,HD}}{\left(\upsilon_3-\upsilon_4\gamma^1_{0,HD}\right)\rho_R\beta_{g_1}}}\\ &\quad\times\sum_{n_3=0}^{m_{g_1}-1}\frac{1}{n_3!\beta_{g_1}^{n_3}}\left(\frac{\gamma^1_{0,HD}}{\left(\upsilon_3-\upsilon_4\gamma^1_{0,HD}\right)\rho_R}\right)^{n_3}.\end{aligned} \tag{D.5}$$

Plugging above values of (D.4) and (D.5) into (D.1) we obtain the final formula.

This is end of proof.

APPENDIX E
PROOF OF PROPOSITION 5

After simple manipulations, we have following equation as

$$\begin{aligned}\Psi_5 = \Pr\Bigg(&\frac{\upsilon_1\rho_S|h_1|^2}{\upsilon_2\rho_S|h_2|^2+1}\geq\gamma^1_{0,HD},\\ &\frac{\upsilon_2\rho_S|h_2|^2}{\upsilon_1\rho_S|k_r|^2+1}\geq\gamma^2_{0,HD}\Bigg).\end{aligned} \tag{E.1}$$

After placing the following variables $y=|h_2|^2$, $z=|k_r|^2$ and performing calculations, we have

$$\Psi_5 = \int_{\frac{\gamma^2_{0,HD}}{\upsilon_2\rho_S}(\upsilon_1\rho_S z+1)}^{\infty}\Omega_1(y)f_y(y)\,dy\int_0^{\infty}f_z(z)\,dz, \tag{E.2}$$

with

$$\begin{aligned}\Omega_1(y) &= 1-F_{|h_1|^2}\left(\frac{\gamma^1_{0,HD}}{\upsilon_1\rho_S}\left(\upsilon_2\rho_S y+1\right)\right)\\ &= e^{-\frac{\gamma^1_{0,HD}(\upsilon_2\rho_S y+1)}{\upsilon_1\rho_S\beta_{h_1}}}\sum_{n=0}^{m_{h_1}-1}\frac{1}{n!\beta_{h_1}^n}\\ &\quad\times\left(\frac{\gamma^1_{0,HD}}{\upsilon_1\rho_S}\right)^n\left(\upsilon_2\rho_S y+1\right)^n\\ &= \sum_{n=0}^{m_{h_1}-1}\sum_{n_1=0}^{n}\binom{n}{n_1}\frac{1}{n!}\left(\frac{\gamma^1_{0,HD}}{\upsilon_1\rho_S\beta_{h_1}}\right)^n\\ &\quad\times\upsilon_2^{n_1}\rho_S^{n_1}e^{-\frac{\gamma^1_{0,HD}}{\upsilon_1\rho_S\beta_{h_1}}}e^{-\frac{\gamma^1_{0,HD}\upsilon_2}{\upsilon_1\beta_{h_1}}y}y^{n_1}.\end{aligned} \tag{E.3}$$

In this case, the last step can be performed by using trinomial expansion [[34], eq. (1.111)]. Plugging (E.3) into (E.2), and after making some manipulations with the help of [[34],

$$\begin{aligned}\Psi_3 &= \Pr\left(\gamma_{R\leftarrow1}\geq\gamma^1_0,\gamma^{pSIC}_{R\leftarrow2}\geq\gamma^2_0\right)\\ &= \sum_{n=0}^{m_{h_1}-1}\sum_{n_1=0}^{n}\sum_{n_2=0}^{n_1}\binom{n}{n_1}\binom{n_1}{n_2}\frac{\upsilon_2^{n_1-n_2}\rho_S^{n_1-n_2}\rho_R^{n_2}}{n!\beta_{h_1}^n}\left(\frac{\gamma^1_0}{\upsilon_1\rho_s}\right)^n\\ &\quad\times\frac{e^{-\frac{\upsilon_2\gamma^1_0\gamma^2_0}{\upsilon_1\upsilon_2\rho_S\beta_{h_1}}-\frac{\gamma^1_0}{\upsilon_1\rho_S\beta_{h_1}}-\frac{\gamma^2_0}{\upsilon_2\rho_S\beta_{h_2}}}}{\Gamma\left(m_{h_2}\right)\beta_{h_2}^{m_{h_2}}}\left(\frac{\gamma^1_0\upsilon_2}{\upsilon_1\beta_{h_1}}+\frac{1}{\beta_{h_2}}\right)^{-n_1+n_2-m_{h_2}}\left(n_1-n_2+m_{h_2}-1\right)!\\ &\quad\times\sum_{n_3=0}^{n_1-n_2+m_{h_2}-1}\sum_{n_4=0}^{n_3}\binom{n_3}{n_4}\frac{{\rho_R}^{n_4}}{n_3!\Gamma\left(m_f\right)\beta_f^{m_f}}\left(\frac{\upsilon_2\gamma^1_0\gamma^2_0}{\upsilon_1\upsilon_2\rho_S\beta_{h_1}}+\frac{\gamma^2_0}{\upsilon_2\rho_S\beta_{h_2}}\right)^{n_3}\\ &\quad\times\left(\frac{\gamma^1_0\rho_R}{\upsilon_1\rho_S\beta_{h_1}}+\left(\frac{\gamma^1_0\upsilon_2}{\upsilon_1}+\frac{1}{\beta_{h_2}}\right)\frac{\gamma^2_0\rho_R}{\upsilon_2\rho_S}+\frac{1}{\beta_f}\right)^{-n_2-n_4-m_f}\Gamma\left(n_2+n_4+m_f\right)\end{aligned} \tag{C.1}$$

eq. (3.381.3), eq. (3.381.4)and eq. (8.352.2)], it is given by

$$\Psi_5 = \sum_{n=0}^{m_{h_1}-1} \sum_{n_1=0}^{n} \binom{n}{n_1} \frac{\upsilon_2^{n_1} e^{-\frac{\gamma^1_{0,HD}}{\upsilon_1 \rho_S \beta_{h_1}}}}{n! \rho_S^{n-n_1}} \left(\frac{\gamma^1_{0,HD}}{\upsilon_1 \beta_{h_1}}\right)^n \times \frac{1}{\Gamma\left(m_{k_r}\right) \beta_{k_r}^{m_{k_r}}} \int_0^{\infty} \Omega_2\left(z\right) z^{m_{k_r}-1} e^{-\frac{z}{\beta_{k_r}}} dz, \quad \text{(E.4)}$$

with

$$\begin{aligned}\Omega_2\left(z\right) &= \int_{\frac{\gamma^2_{0,HD}}{\upsilon_2 \rho_S}(\upsilon_1 \rho_S z+1)}^{\infty} e^{-\frac{\gamma^1_{0,HD}\upsilon_2}{\upsilon_1 \beta_{h_1}} y} y^{n_1} f_y\left(y\right) dy \\ &= \frac{{\vartheta_1}^{-\tau_2}}{\Gamma\left(m_{h_2}\right) \beta_{h_2}^{m_{h_2}}} \Gamma\left(\tau_2, \frac{\vartheta_1 \gamma^2_{0,HD}}{\upsilon_2 \rho_S}\left(\upsilon_1 \rho_S z+1\right)\right) \\ &= \frac{\Gamma\left(\tau_2\right) {\vartheta_1}^{-\tau_2}}{\Gamma\left(m_{h_2}\right) \beta_{h_2}^{m_{h_2}}} e^{-\frac{\vartheta_1 \gamma^2_{0,HD}}{\upsilon_2 \rho_S}} \sum_{n_2=0}^{\tau_2-1} \sum_{n_3=0}^{n_2} \binom{n_2}{n_3} \frac{1}{n_2!} \\ &\quad \times \left(\frac{\vartheta_1 \gamma^2_{0,HD}}{\upsilon_2 \rho_S}\right)^{n_2} \upsilon_1^{n_3} \rho_S^{n_3} e^{-\frac{\vartheta_1 \gamma^2_{0,HD} \upsilon_1 z}{\upsilon_2}} z^{n_3}, \end{aligned} \quad \text{(E.5)}$$

where $\tau_2 \triangleq n_1 + m_{h_2}$ and $\vartheta_1 \triangleq \frac{\gamma^1_{0,HD}\upsilon_2}{\upsilon_1 \beta_{h_1}} + \frac{1}{\beta_{h_2}}$.

Finally, replacing (E.5) into (E.4), we have

$$\begin{aligned}\Psi_5 &= e^{-\frac{\gamma^1_{0,HD}}{\upsilon_1 \rho_S \beta_{h_1}}} \sum_{n=0}^{m_{h_1}-1} \sum_{n_1=0}^{n} \binom{n}{n_1} \frac{\upsilon_2^{n_1}}{n! \rho_S^{n-n_1}} \left(\frac{\gamma^1_{0,HD}}{\upsilon_1 \beta_{h_1}}\right)^n \\ &\quad \times \frac{\Gamma\left(\tau_2\right) {\vartheta_1}^{-\tau_1} e^{-\frac{\vartheta_1 \gamma^2_{0,HD}}{\upsilon_2 \rho_S}}}{\Gamma\left(m_{h_2}\right) \beta_{h_2}^{m_{h_2}}} \sum_{n_2=0}^{\tau_2-1} \sum_{n_3=0}^{n_2} \binom{n_2}{n_3} \frac{1}{n_2!} \\ &\quad \times \left(\frac{\vartheta_1 \gamma^2_{0,HD}}{\upsilon_2 \rho_S}\right)^{n_2} \frac{\upsilon_1^{n_3} \rho_S^{n_3}}{\Gamma\left(m_{k_r}\right) \beta_{k_r}^{m_{k_r}}} \\ &\quad \times \Gamma\left(n_3 + m_{k_r}\right) \left(\frac{\upsilon_1 \vartheta_1 \gamma^2_{0,HD}}{\upsilon_2} + \frac{1}{\beta_{k_r}}\right)^{-n_3-m_{k_r}}. \end{aligned} \quad \text{(E.6)}$$

In HD mode, because $\gamma_{U_4 \leftarrow 1}$ and $\gamma_{U_4}^{ipSIC}$ are unchanged compared to the full duplex mode, we have

$$\begin{aligned}\Psi_6 &= e^{-\frac{\gamma^2_{0,HD}}{\upsilon_4 \rho_R \beta_{g_2}}} \sum_{n_6=0}^{m_{g_2}-1} \sum_{n_7=0}^{n_6} \binom{n_6}{n_7} \frac{\upsilon_3^{n_7} \rho_R^{n_7}}{n_6! \beta_{g_2}^{n_6}} \left(\frac{\gamma^2_{0,HD}}{\upsilon_4 \rho_R}\right)^{n_6} \\ &\quad \times \frac{1}{\Gamma\left(m_{k_2}\right) \beta_{k_2}^{m_{k_2}}} \left(\frac{\gamma^2_{0,HD}\upsilon_3}{\upsilon_4 \beta_{g_2}} + \frac{1}{\beta_{k_2}}\right)^{-n_7-m_{k_2}} \\ &\quad \times \Gamma\left(n_7 + m_{k_2}, \frac{\gamma^2_{0,HD}\upsilon_3 \vartheta_2}{\upsilon_4 \beta_{g_2}} + \frac{\vartheta_2}{\beta_{k_2}}\right) \\ &\quad + \frac{1}{\Gamma\left(m_{g_2}\right)} \Gamma\left(m_{g_2}, \frac{\gamma^1_{0,HD}}{\upsilon_3 \rho_R \beta_{g_2} - \upsilon_4 \rho_R \gamma^1_{0,HD} \beta_{g_2}}\right) \\ &\quad \times \left(1 - \frac{1}{\Gamma\left(m_{k_2}\right)} \Gamma\left(m_{k_2}, \frac{\vartheta_2}{\beta_{k_2}}\right)\right), \end{aligned} \quad \text{(E.7)}$$

This is end of proof.

REFERENCES

[1] X. Li, J. Li, and L. Li, "Performance analysis of impaired SWIPT NOMA relaying networks over imperfect weibull channels," *IEEE Syst. J.*, vol. 14, no. 1, pp. 669–672, Mar. 2020.

[2] X. Li, M. Liu, D. Deng, J. Li, C. Deng, and Q. Yu, "Power beacon assisted wireless power cooperative relaying using NOMA with hardware impairments and imperfect CSI," *AEU-Int. J. Electron. Commun.*, vol. 108, pp. 275–286, Aug. 2019.

[3] L. Zhang, M. Xiao, G. Wu, M. Alam, Y.-C. Liang, and S. Li, "A survey of advanced techniques for spectrum sharing in 5G networks," *IEEE Wireless Commun.*, vol. 24, no. 5, pp. 44–51, Oct. 2017.

[4] D.-T. Do, A.-T. Le, and B. M. Lee, "NOMA in cooperative underlay cognitive radio networks under imperfect SIC," *IEEE Access*, vol. 8, pp. 86180–86195, 2020.

[5] D.-T. Do and M.-S. Van Nguyen, "Device-to-device transmission modes in NOMA network with and without wireless power transfer," *Comput. Commun.*, vol. 139, pp. 67–77, May 2019.

[6] D.-T. Do and A.-T. Le, "NOMA based cognitive relaying: Transceiver hardware impairments, relay selection policies and outage performance comparison," *Comput. Commun.*, vol. 146, pp. 144–154, Oct. 2019.

[7] T.-L. Nguyen and D.-T. Do, "Power allocation schemes for wireless powered NOMA systems with imperfect CSI: An application in multiple antenna-based relay," *Int. J. Commun. Syst.*, vol. 31, no. 15, p. e3789, Oct. 2018.

[8] Z. Wei, J. Yuan, D. W. K. Ng, M. Elkashlan, and Z. Ding, "A survey of downlink non-orthogonal multiple access for 5G wireless communication networks," 2016, *arXiv:1609.01856*. [Online]. Available: http://arxiv.org/abs/1609.01856

[9] F. Wei, T. Zhou, T. Xu, and H. Hu, "Modeling and analysis of two-way relay networks: A joint mechanism using NOMA and network coding," *IEEE Access*, vol. 7, pp. 152679–152689, 2019.

[10] W. Zhao, R. She, and H. Bao, "Security energy efficiency maximization for two-way relay assisted cognitive radio NOMA network with self-interference harvesting," *IEEE Access*, vol. 7, pp. 74401–74411, 2019.

[11] W. Zhao, R. She, and H. Bao, "Energy efficiency maximization for two-way relay assisted CR-NOMA system based on SWIPT," *IEEE Access*, vol. 7, pp. 72062–72071, 2019.

[12] D.-T. Do, A.-T. Le, and A. B. M. Lee, "On performance analysis of underlay cognitive radio-aware hybrid OMA/NOMA networks with imperfect CSI," *Electronics*, vol. 8, no. 7, p. 819, Jul. 2019.

[13] Z. Ding, M. Peng, and H. V. Poor, "Cooperative non-orthogonal multiple access in 5G systems," *IEEE Commun. Lett.*, vol. 19, no. 8, pp. 1462–1465, Aug. 2015.

[14] M. Xu, F. Ji, M. Wen, and W. Duan, "Novel receiver design for the cooperative relaying system with non-orthogonal multiple access," *IEEE Commun. Lett.*, vol. 20, no. 8, pp. 1679–1682, Aug. 2016.

[15] J.-B. Kim and I.-H. Lee, "Capacity analysis of cooperative relaying systems using non-orthogonal multiple access," *IEEE Commun. Lett.*, vol. 19, no. 11, pp. 1949–1952, Nov. 2015.

[16] M. F. Kader, M. B. Shahab, and S. Y. Shin, "Exploiting non-orthogonal multiple access in cooperative relay sharing," *IEEE Commun. Lett.*, vol. 21, no. 5, pp. 1159–1162, May 2017.

[17] X.-X. Nguyen and D.-T. Do, "Maximum harvested energy policy in full-duplex relaying networks with SWIPT," *Int. J. Commun. Syst.*, vol. 30, no. 17, p. e3359, Nov. 2017.

[18] X.-X. Nguyen and D.-T. Do, "Optimal power allocation and throughput performance of full-duplex DF relaying networks with wireless power transfer-aware channel," *EURASIP J. Wireless Commun. Netw.*, vol. 2017, no. 1, p. 152, Dec. 2017.

[19] M. F. Sohail, C. Y. Leow, and S. Won, "Non-orthogonal multiple access for unmanned aerial vehicle assisted communication," *IEEE Access*, vol. 6, pp. 22716–22727, 2018.

[20] Y. Zeng, R. Zhang, and T. J. Lim, "Wireless communications with unmanned aerial vehicles: Opportunities and challenges," *IEEE Commun. Mag.*, vol. 54, no. 5, pp. 36–42, May 2016.

[21] T. Hou, Y. Liu, Z. Song, X. Sun, and Y. Chen, "Multiple antenna aided NOMA in UAV networks: A stochastic geometry approach," *IEEE Trans. Commun.*, vol. 67, no. 2, pp. 1031–1044, Feb. 2019.

[22] N. Rupasinghe, Y. Yapıcı, İ. Güvenç, and Y. Kakishima, "Non-orthogonal multiple access for mmWave drone networks with limited feedback," *IEEE Trans. Commun.*, vol. 67, no. 1, pp. 762–777, Jan. 2019.

[23] N. Senadhira, S. Durrani, X. Zhou, N. Yang, and M. Ding, "Uplink NOMA for cellular-connected UAV: Impact of UAV trajectories and altitude," *IEEE Trans. Commun.*, vol. 68, no. 8, pp. 5242–5258, Aug. 2020, doi: 10.1109/TCOMM.2020.2995373.
[24] X. Li, Q. Wang, Y. Liu, T. A. Tsiftsis, Z. Ding, and A. Nallanathan, "UAV-aided multi-way NOMA networks with residual hardware impairments," *IEEE Wireless Commun. Lett.*, vol. 9, no. 9, pp. 1538–1542, Sep. 2020, doi: 10.1109/LWC.2020.2996782.
[25] T. Z. H. Ernest, A. S. Madhukumar, R. P. Sirigina, and A. K. Krishna, "NOMA-aided UAV communications over correlated rician shadowed fading channels," *IEEE Trans. Signal Process.*, vol. 68, pp. 3103–3116, 2020.
[26] L. Wang, B. Hu, S. Chen, and J. Cui, "UAV-enabled reliable mobile relaying based on downlink NOMA," *IEEE Access*, vol. 8, pp. 25237–25248, 2020.
[27] X. Yue, Y. Liu, S. Kang, A. Nallanathan, and Y. Chen, "Modeling and analysis of two-way relay non-orthogonal multiple access systems," *IEEE Trans. Commun.*, vol. 66, no. 9, pp. 3784–3796, Sep. 2018.
[28] M. F. Kader, S. Y. Shin, and V. C. M. Leung, "Full-duplex non-orthogonal multiple access in cooperative relay sharing for 5G systems," *IEEE Trans. Veh. Technol.*, vol. 67, no. 7, pp. 5831–5840, Jul. 2018.
[29] Y. Saito, Y. Kishiyama, A. Benjebbour, T. Nakamura, A. Li, and K. Higuchi, "Non-orthogonal multiple access (NOMA) for cellular future radio access," in *Proc. IEEE 77th Veh. Technol. Conf. (VTC Spring)*, Jun. 2013, pp. 1–5.
[30] D.-T. Do, M.-S. V. Nguyen, A.-T. Le, J. Zhang, and K. Rabie, "Joint FullDuplex and roadside unit selection for NOMA-enabled V2X communications: Ergodic rate performance," *IEEE Access*, vol. 8, pp. 140348–140360, 2020.
[31] D. Zhang, Y. Liu, L. Dai, A. K. Bashir, A. Nallanathan, and B. Shim, "Performance analysis of FD-NOMA-based decentralized V2X systems," *IEEE Trans. Commun.*, vol. 67, no. 7, pp. 5024–5036, Jul. 2019.
[32] J. Montalban, P. Scopelliti, M. Fadda, E. Iradier, C. Desogus, P. Angueira, M. Murroni, and G. Araniti, "Multimedia multicast services in 5G networks: Subgrouping and non-orthogonal multiple access techniques," *IEEE Commun. Mag.*, vol. 56, no. 3, pp. 91–95, Mar. 2018.
[33] P. K. Sharma and D. I. Kim, "UAV-enabled downlink wireless system with non-orthogonal multiple access," in *Proc. IEEE Globecom Workshops (GC Wkshps)*, Singapore, Dec. 2017, pp. 1–6.
[34] I. S. Gradshteyn and I. M. Ryzhik, *Table of Integrals, Series and Products*, 7th ed. New York, NY, USA: Academic, 2007.

DINH-THUAN DO (Senior Member, IEEE) received the B.S., M.Eng., and Ph.D. degrees from Vietnam National University (VNU-HCM), in 2003, 2007, and 2013, respectively, all in communications engineering.

Prior to joining Ton Duc Thang University, he was a Senior Engineer with VinaPhone Mobile Network, from 2003 to 2009. He has published over 75 SCI/SCIE journal articles, one sole author book, and five book chapters. His research interests include signal processing in wireless communications networks, cooperative communications, non-orthogonal multiple access, full-duplex transmission, and energy harvesting. He was a recipient of the Golden Globe Award from the Vietnam Ministry of Science and Technology, in 2015 (Top 10 Excellent Young Scientists Nationwide). He has been serving as an Associate Editor for six journals, in which main journals are *EURASIP Journal on Wireless Communications and Networking*, *Computer Communications* (Elsevier), and the *KSII Transactions on Internet and Information Systems*.

TU-TRINH THI NGUYEN received the B.Sc. degree in electrical-electronics engineering from the Industrial University of Ho Chi Minh City, Vietnam, in 2018. She intends to pursue her study in the Ph.D. degree. She is currently working with the WICOM Laboratory, which has lead by Dr. Thuan. Her research interests include signal processing in wireless communications networks, NOMA, and relaying networks.

TU N. NGUYEN (Senior Member, IEEE) received the Ph.D. degree in electronic engineering from the National Kaohsiung University of Science and Technology (formerly, National Kaohsiung University of Applied Sciences), Kaohsiung, Taiwan, in 2016. He was a Postdoctoral Associate with the Department of Computer Science and Engineering, University of Minnesota-Twin Cities, in 2017. Prior to joining the University of Minnesota, he joined the Missouri University of Science and Technology as a Postdoctoral Researcher with the Intelligent Systems Center, in 2016. He is currently an Assistant Professor with the Department of Computer Science, Purdue University Fort Wayne, Fort Wayne, IN, USA. His research interests include design and analysis of algorithms, network science, cyber-physical systems, and cybersecurity. He was a Technical Program Committee Member for more than 70 premium conferences in the areas of network and communication, such as INFOCOM, Globecom, ICC, and RFID. He was the TPC Co-Chair of the NAFOSTED Conference on Information and Computer Science (NICS) 2019, SoftCOM (25th), and the EAI International Conference on Context-Aware Systems and Applications (ICCASA) 2017; the Publicity Chair of the International Conference on Awareness Science and Technology (iCAST) 2017 and BigDataSecurity 2017; and the Track Chair of ACT 2017. He has been an Associate Editor of IEEE Access and the *EURASIP Journal on Wireless Communications and Networking* since 2017. He is also on the Editorial Board of the *Cybersecurity* journal, the *Internet Technology Letters* since 2017, the *International Journal of Vehicle Information and Communication Systems* since 2017, the *International Journal of Intelligent Systems Design and Computing* since 2017, and *IET Wireless Sensor Systems* since 2017.

XINGWANG LI (Senior Member, IEEE) received the B.Sc. degree from Henan Polytechnic University, in 2007, the M.Sc. degree from the University of Electronic Science and Technology of China in 2010, and the Ph.D. degree from the Beijing University of Posts and Telecommunications, in 2015. From 2010 to 2012, he has worked with Comba Telecom Ltd., Guangzhou, China, as an Engineer. He was a Visiting Scholar with the State Key Laboratory of Networking and Switching Technology, Beijing University of Posts and Telecommunications, from 2016 to 2018. He spent one year as a Visiting Scholar with Queen's University Belfast, Belfast, U.K., from 2017 to 2018. He is currently an Associate Professor with the School of Physics and Electronic Information Engineering, Henan Polytechnic University, Jiaozuo, China. His research interests include MIMO communication, cooperative communication, hardware constrained communication, non-orthogonal amultiple access, physical layer security, unmanned aerial vehicles, and the Internet of Things. He has served as a TPC member for IEEE/CIC International Conference on Communications in China (ICCC'2019) and IEEE Global Communications Conference 2018 (Globecom'18). He is currently an Editor on the Editorial Board of IEEE Access, *Computer Communications*, and the *KSII Transactions on Internet and Information Systems*.

MIROSLAV VOZNAK (Senior Member, IEEE) received the Ph.D. degree in telecommunications from the Faculty of Electrical Engineering and Computer Science, VSB–Technical University of Ostrava, in 2002, and the Habilitation degree, in 2009. He was appointed as a Full Professor in electronics and communications technologies, in 2017. He is the author or a coauthor of more than 100 articles in SCI/SCIE journals. His research interests include information and communication technologies, especially on the Quality of Service and Experience, network security, wireless networks, and big data analytics. He has served as a member of editorial boards for several journals, including *Sensors*, the *Journal of Communications*, *Elektronika Ir Elektrotechnika*, and *Advances in Electrical and Electronic Engineering*.